Development of a CAN Based Electric Vehicle Control System

By

Stephen A. Vincent

Submitted to the graduate degree program in Mechanical Engineering and the Graduate Faculty of the University of Kansas in partial fulfillment of the requirements for the degree of Master of Science.

_____

Chairperson Dr. Terry Faddis

_____

Dr. Lorin Maletsky

_____

Dr. Bedru Yimer

Date Defended: June 24, 2014

The Thesis Committee for Stephen A. Vincent

certifies that this is the approved version of the following thesis:

Development of a CAN Based Electric Vehicle Control System

_____

Chairperson Dr. Terry Faddis

Date approved: June 24, 2014

Abstract

The Intelligent Systems and Automation Lab (ISAL) at the University of Kansas has been working on developing new electric vehicle drivetrain and battery technology using an electric bus as a development platform. In its preexisting state the bus featured an unreliable control system to manage load control and drive enable functions. As a result this thesis presents the design of a Controller Area Network (CAN) based control system to be used as a replacement for the existing system. The use of this new system will allow for easy expansion, higher efficiency and greater reliability in further developing the ISAL electric bus concept vehicle.

Controller Area Network protocol allows the system to easily implement smart features allowing multiple modules to work together as well as reduce the overall wiring complexity of the control system. CAN networks utilize a single twisted pair cable and differential transmission to reliably transmit data to all modules featured in the control system. Additionally, because CAN is a common network protocol used in automotive electronics it will be easy to interface with other existing automotive electronics.

This thesis shows the development of six different CAN modules as well as a proposed implementation for the complete system. Developed modules include an Interior Lighting Module, Headlights and Accessories Load Module, Accelerator Pedal Sensor Module, Battery Voltage Sensor Module, Input Module, and Speed Sensor and Display Module. Modules serve the purpose of reading sensors, controlling electric loads and displaying pertinent information to the driver. A prototype of this system featuring one of each module has been created for display and test purposes and is fully functional.

1.0 Project History/Background

Electric vehicles have briefly emerged throughout history several times only to return back to relative obscurity. Low expectations for range combined with the lack of reliability accompanying early steam and gasoline powered vehicles helped electric vehicles gain popularity during the early 1900s [1]. Later improvements in gasoline vehicle performance along with increased reliability resulted in a sharp decline of electric vehicle popularity. Much later, in the 1960s, interest in electric vehicles re-emerged due to rising oil prices and concerns about the output of harmful emissions from gasoline powered vehicles. Later regulations required percentages of vehicle sales to include zero-emission vehicles. Once again low performance, particularly range, resulted in the failure of the electric vehicle to grab a legitimate market share. In recent years battery technology has advanced to a point where electric vehicles have respectable ranges and low charging times [2]. Emergence of new battery technology along with the commercially successful Tesla model S have shown that electric vehicle technology may have finally reached a point where it can become a commercially viable alternative to gasoline powered automobiles. As a result the University of Kansas Intelligent Systems and Automation Lab is working to help benchmark and improve electric vehicle efficiency using their electric bus concept. My contribution is the development and testing of a Controller Area Network based electric vehicle control system composed of six different networkable modules.

Many don't realize that during the infancy of automobiles there was a time when electric vehicles were a prominent alternative to gasoline and steam powered options. In 1900 there were 4,192 vehicles produced in the United States, 28% featured an electric-powered drivetrain [1]. That same year at the New York Auto Show there were more electric vehicles on display than any other type of vehicle. This popularity increased until electric vehicle production peaked

in 1913 followed by a rapid decline [1]. Refinement of the once clunky internal combustion engine coupled with a desire for increased range and speed provided gasoline powered automobiles with a meteoric rise in popularity [2]. Refueling gasoline powered vehicles was also relatively simple compared to operating the expensive, difficult to use charging setups available for electric vehicles at that time. Many early electric vehicles relied on custom charging setups that were often run only by electricians [1]. By 1920 the electric vehicle was mostly dead, with the exception of a few niche markets.

Increasing gasoline prices along with increased concerns about vehicle emissions led to a resurgence in interest toward electric vehicles. Many electric vehicles being developed at the time were simply electric conversions of existing gasoline powered vehicles. In the mid 1960's both General Motors and Ford began developing purpose built electric vehicles in an effort to increase performance. While much higher performance than their predecessors, these vehicles still failed to come anywhere close to the performance of a gasoline powered automobile [2]. A 1990 California Air Resources Board (CARB) regulation called for 2% of light duty vehicles produced by manufactures selling 35,000 automobiles or more per year to be zero emission vehicles [3]. As a result major automakers began developing electric vehicles including the General Motors EV1, Ford TH!NK City, Nissan Hypermini, and Toyota RAV4 Electric [2]. Even these vehicles suffered from poor performance when compared to a gasoline powered vehicle. In 1996 when General Motors delivered the first of their EV1 mass-produced electric vehicles the maximum range was only 90 miles [3]. As a result, this new round of electric vehicles, most of which were relatively expensive, sold poorly and considered by many to be a failure.

Recent technological developments, including high energy density lithium ion battery packs, and high efficiency drivetrains have brought electric vehicle performance to a level that many feel could make them a successful alternative to gasoline powered vehicles. The 2006 announcement of the Tesla Roadster, which would go on sale in 2008, showed just how far electric vehicle performance had improved. With a US EPA stated range of 244 miles and the ability to go from 0 to 60 miles per hour in 3.7 seconds the performance was on par or exceeding that of many gasoline powered sports cars. Additionally, a range of 244 miles exceeds that of the average commuter's daily drive limiting the owner's range-anxiety. The release of several high performance electric cars, along with renewed government interest in electric vehicles, has sparked further research in developing electric vehicle technology. The University of Kansas has been working to develop and benchmark new battery and drivetrain technologies using its Electric Bus concept vehicle. As part of that system, I developed and tested a networked smart control system designed to increase reliability and efficiency of all peripherals and parasitic loads. Specifically, the system I developed contains the six networkable modules discussed in this thesis.

2.0 CAN Protocol Overview

Most vehicles feature a number of different electronics modules which need to be networked for the vehicle to operate properly. Prior to development of the Controller Area Network (CAN), bus modules generally featured individual connections to every other module with which they interfaced. CAN bus was developed by Robert Bosch in the mid 1980's [4] to replace car networks with a simpler, lower weight and lower cost alternative. Using a CAN bus network every module can be networked to every other module with only a single connection to a common twisted pair connection terminated at either end with 120 ohm resistors [5].

Prior to the development of CAN bus, modules often had a wired connection to every single module that they communicated with. The result of this was often complex, heavy wiring harnesses and large amounts of processing power dedicated strictly to communication. Figures 2.1 and 2.2 show the wiring simplification offered in this control system. Simplification would be even greater in many electrical vehicles because of the large number of modules that must interface with each other.

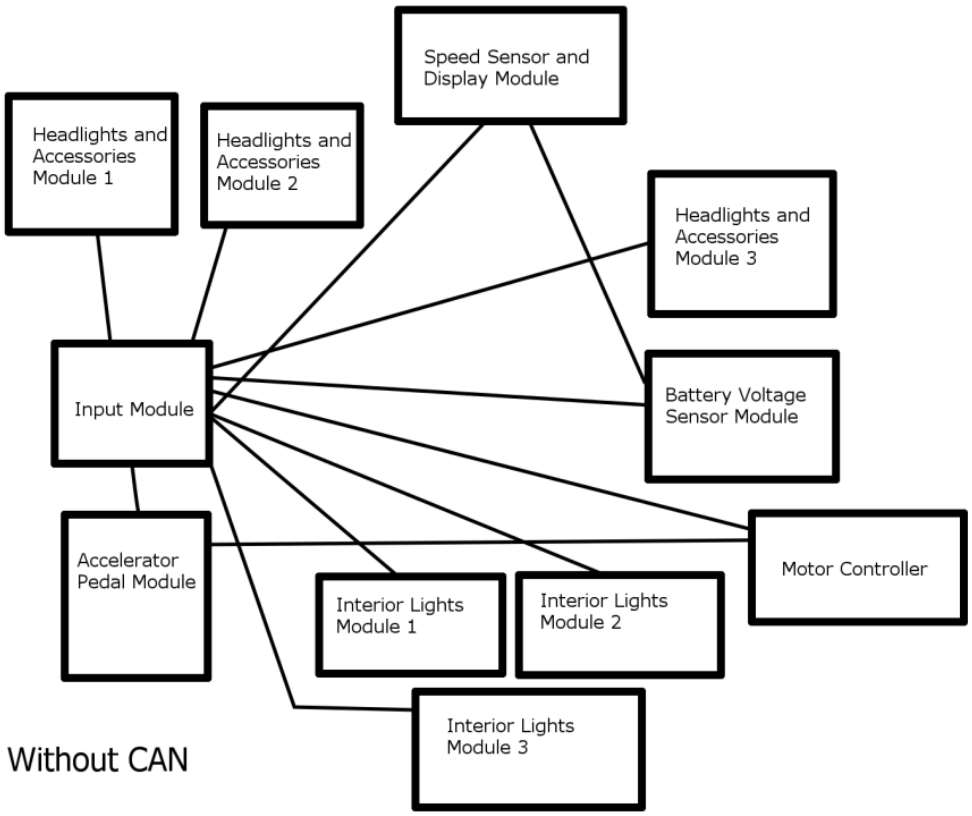

Figure 2.1: Wiring Diagram without Controller Area Network

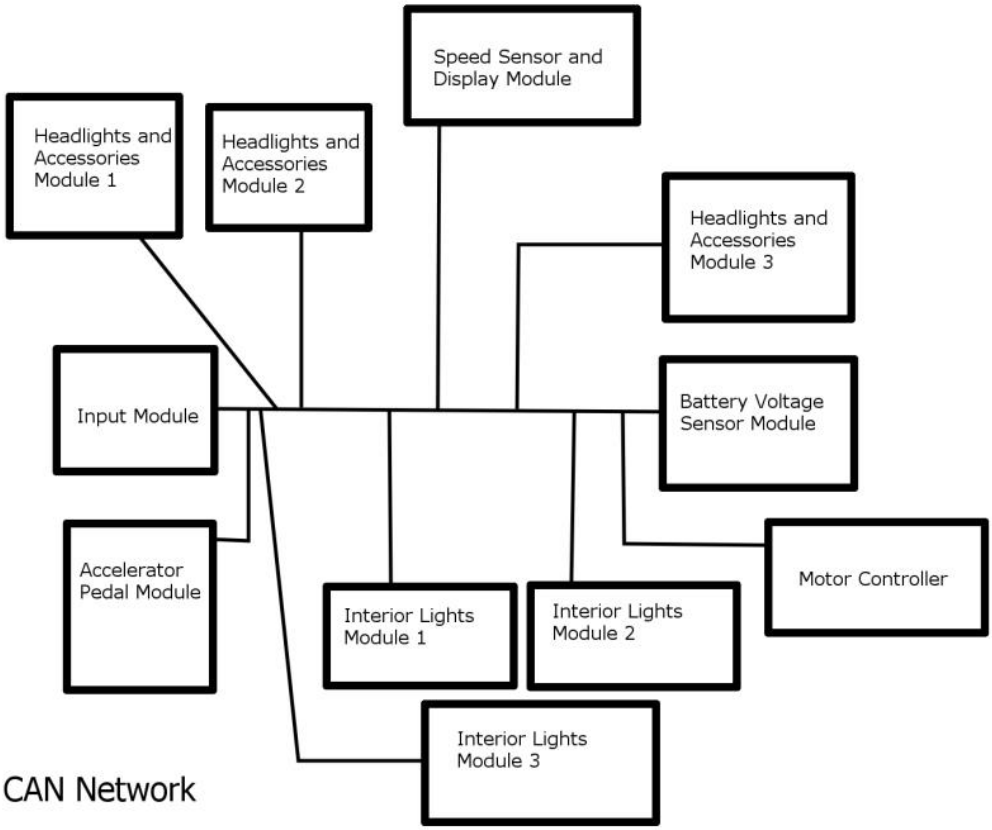

Figure 2.2: Wiring Diagram with Controller Area Network

Standard serial communication typically sends a digital high state of 3.3 V or 5 V for a 1 and a digital low state of 0v for a 0. Over long distances this can be affected negatively by electrical noise, which is frequently present in vehicles. CAN bus utilizes a differential pair that monitors the difference between the state of a twisted pair of wires. Since it is likely that electrical noise will affect both wires in the twisted pair equally the differential between them is likely to be affected less by electrical noise. In particular CAN bus uses a differential system where a 1 is sent when the twisted pair is in the recessive state and a 0 is sent when the pair is in the dominant state. The recessive state occurs when both the high and low side of the CAN bus are at a 2.5 V potential (Fig. 2.3). A dominant state occurs with a 3.3 V CAN transceiver when

the voltage of the high side of the bus is at 3.5v and the low side is at 1.5v creating a 2v differential between the high and low side [6]. In a differential system if electrical noise causes both voltages to either go up or down the difference between them will still remain the same and the transmission will not be altered.

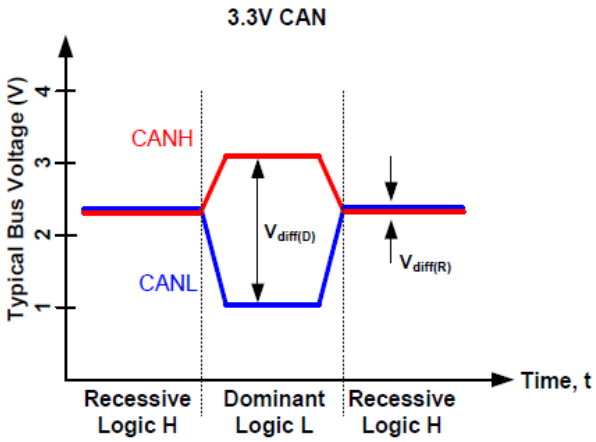

Figure 2.3: Differential Signal Voltages [6]

CAN networks operating in high speed mode are also capable of transmitting data up to 1 Mbit/second if the bus length is 40 meters or less [5]. CAN networks are also capable of error checking and can feature a high number of nodes due to their 11 bits of data available for CAN IDs [4].

In addition to simplified wiring, CAN bus networks are message based and therefore every message is simply transmitted to the CAN bus rather than a specifically addressed module. A benefit of this is that every module attached to the CAN bus is capable of receiving messages from every other module attached to the bus. A result of this is a system that's much simpler to upgrade and add features to without the addition of complicated wiring. Modules must then determine whether or not to discard or use each message that they receive [4]. This makes it

particularly easy to send sensor data to a number of different modules as well as implement several identical modules. The control system designed for this thesis employs multiple interior lighting modules all of which are identical in hardware and software and react to the same messages sent over the CAN bus.

According to the CAN protocol each message must contain certain data and structure as seen in figure 2.4.

SOF	11 bit CAN ID	RTR	IDE	R0	DLC	Data	CRC	ACK	EOF	IFS

Table 2.1: CAN Message Structure

SOF: (1 bit) Start of Frame bit signals the start of a frame by first sending dominant bit. This bit helps all of the modules synchronize after being in an idle state

11 bit CAN ID: (11 bits) binary identifier. Lower values have a higher priority

RTR: (1 bit): Remote Transmission Request. This bit is dominant when information is needed from another node

IDE: (1 bit): Identifier extension

R0: (1 bit) Reserved bit: this is reserved for possible future amendments to the standard

DLC: (4 bits) Data Length Code: this is a 4 bit number that establishes how many bits of data will be transmitted

DATA: (8 bits) The 8 bits of data transferred to the bus are stored here.

CRC: (16 bits) Cyclic Redundancy Check, this contains a checksum of preceding application data for error detection

ACK: (2 bits) this contains an acknowledgement bit and a delimiter bit. When the original message is sent the first bit is sent as recessive. When each node receives the message if properly received, it will overwrite this bit with a dominant bit. This verifies the integrity of data sent over the CAN bus.

EOF: (7 bits) These 7 bits mark the end of frame of communication

IFS: (7 bits) These 7 bits are known as the inter-frame space. They provide the necessary time for a can controller to move the next message into the buffer. [5]

Most microcontrollers are not capable of directly interfacing with a CAN bus network. Microcontrollers with integrated CAN controllers do exist, however for this system a standalone CAN controller was used. The purpose of a CAN controller is to act as an interface with the microcontroller that will utilize the CAN message protocol, store messages and determine when to accept and reject messages on the CAN bus. Utilizing a CAN controller frees up microcontroller resources for other functions rather than CAN implementation. This system uses the Microchip MCP2515 Can controller IC [7] as its CAN controller which is connected to the CAN bus through a Texas Instruments SN65HVD230 CAN transceiver IC [8] (Figure 2.5). A CAN transceiver allows the CAN controller to send data over a differential bus helping to reduce the effects of noise on transmission. The SN65HVD230 3.3 V transceiver was used over a 5v transceiver due to its ability to reduce node power by as much as 50% [6].

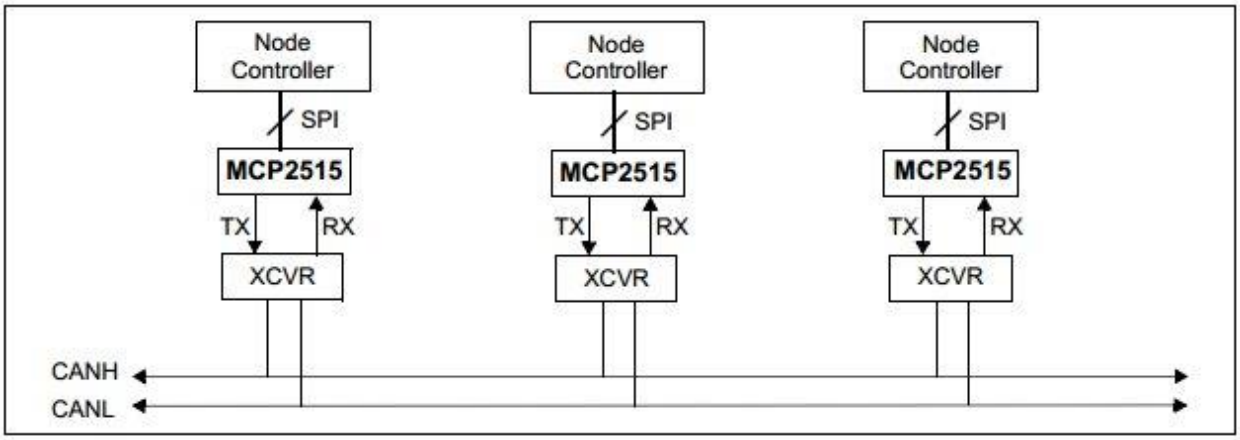

Figure 2.5: Example System Implementation [7]

Since each module only requires a connection to a 9-16v DC power supply as well as a connection to the CAN bus, module placement is much more flexible than with an analog system. In order to reduce the amount of overall wiring, modules are placed near components that they interface with as can be seen in figure 2.6 and Table 2.1

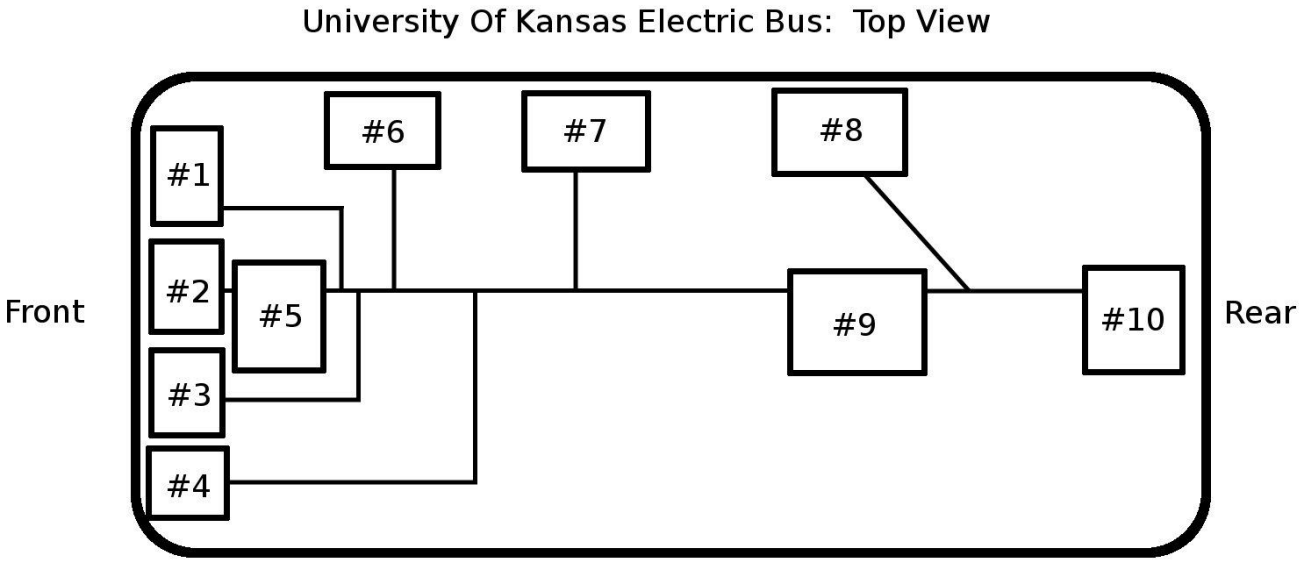

Figure 2.6: Bus Node Layout

Node #	Node Name
1	Headlights and Accessories Module #1
2	Headlights and Accessories Module #2
3	Accelerator Pedal Sensor Module
4	Speed Sensor/Display Module
5	Input Module
6	Interior Lighting Module #1
7	Interior Lighting Module #2
8	Interior Lighting Module #3
9	Battery Voltage Sensor Module
10	Headlights and Accessories Module #3

Table 2.2: Module Allocation

3.0 Interior Lighting Module

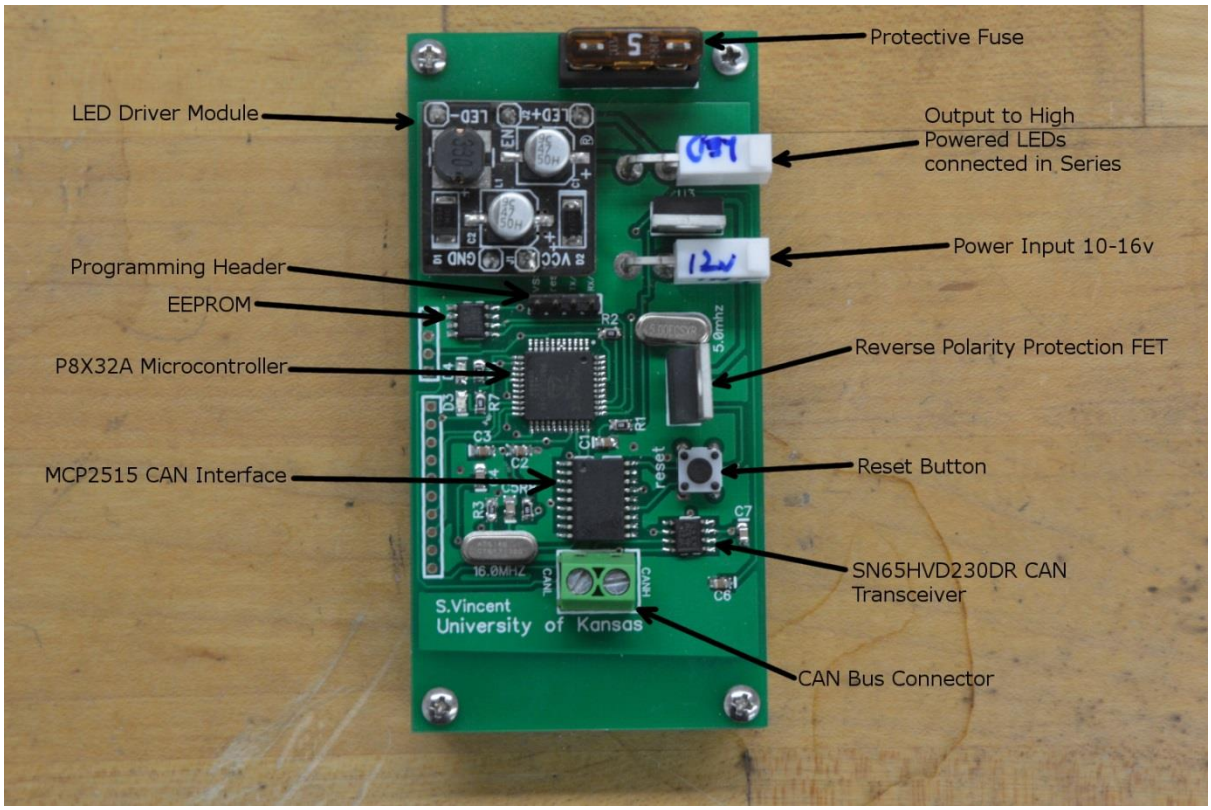

Figure 3.1: Interior Lights Module

3.1 Interior Lighting Module Overview

Interior lighting is facilitated by CAN bus networked MCU controlled modules (Fig. 3.1). Each module is capable of powering up to three one watt high-intensity LEDs connected in series. This system is much more efficient than the bus's preexisting fluorescent lighting system. In addition to offering much higher efficiency this interior lighting module offers greater functionality over the preexisting system due to its CAN bus connectivity. System connectivity can be seen in the flowchart featured in figure 3.2.

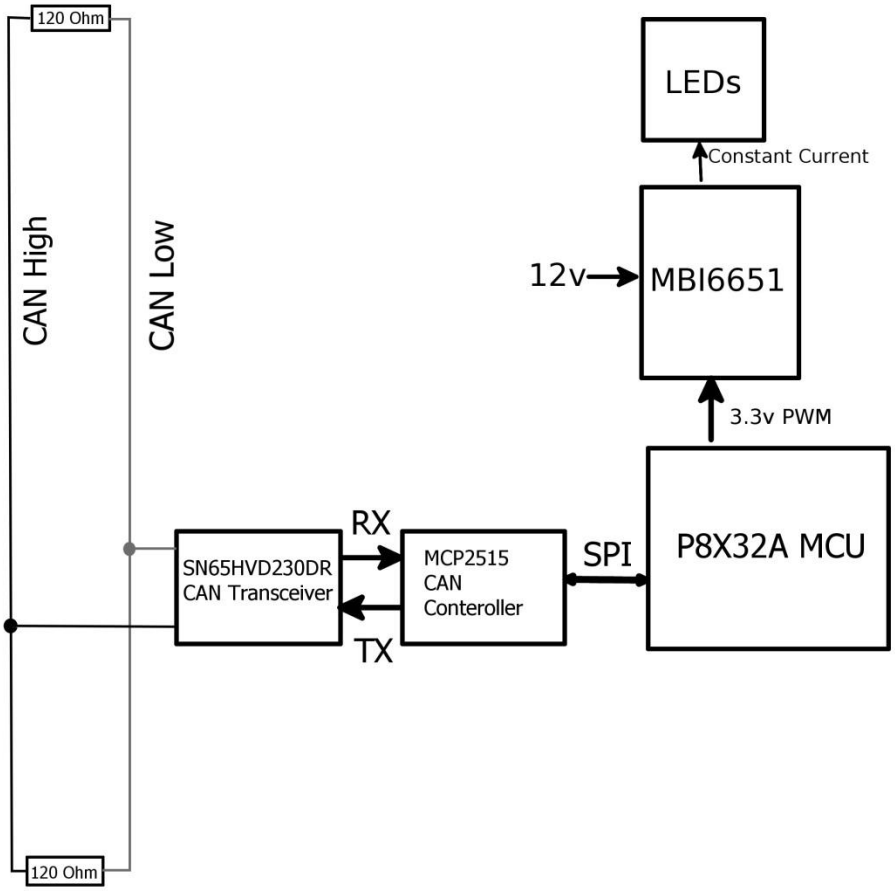

Figure 3.2: Interior Lighting Module Flowchart

3.2 Interior Lighting Module Architecture

The LED driver used in this system is powered by a Macroblock MBI6651 Constant Current Step-Down LED driver integrated circuit [9]. Each integrated circuit can be used with anywhere from 1-6 LEDs and features dimming capabilities controlled via pulse width modulation at either a 3.3 V or 5 V logic level. Each Macroblock IC is placed on the underside of a pre-configured LED module and is configured using the schematic shown in figure 3.3.

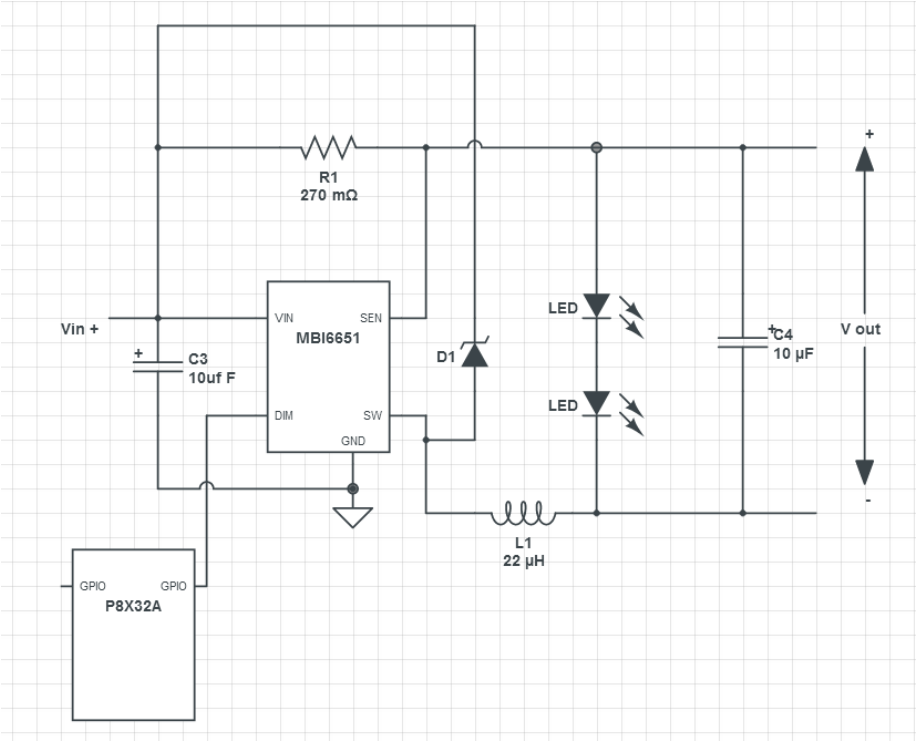

Figure 3.3: LED Driver Schematic

Using the configuration shown in Figure 3.3 the driver will output a constant current of 370 ma making it suitable for use with 1 watt high intensity LEDs. The module itself is capable of driving up to six of these LEDs , however when operating with an input voltage of 12 V it is

limited to three LEDs per module. Since each 1 watt LED is capable of outputting 90 lumens at full brightness [10] a system with six of these modules will provide nearly the same level of light as the previous fluorescent lighting system.

3.3 Comparison with Preexisting Lighting System

The preexisting system featured on the bus contained three fluorescent light fixtures on each side of the bus totaling six fixtures as seen in figure 3.4.

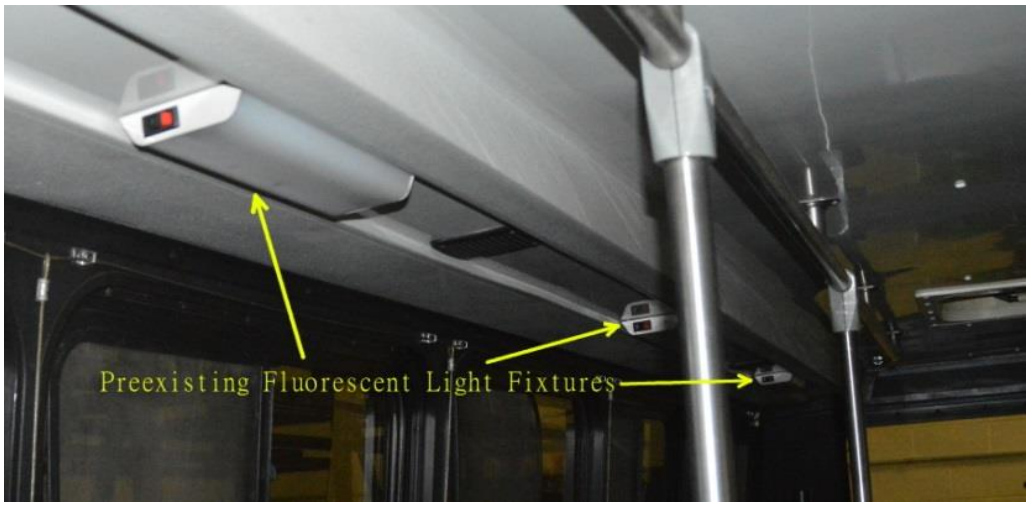

Figure 3.4: Preexisting Light Fixture Placement

Figure 3.5: Individual Preexisting light fixture

Each fixture from the preexisting system housed an f8T5CW fluorescent bulb seen in figure 3.5 and was controlled via analog circuitry allowing only simple on off control. Individual fixtures in the previous system could be controlled using a switch on each fixture as well as total system control via a master switch featured at the front of the bus. Due to the series wiring of switches in the previous system this means that both the individual fixture switch and the master switch must be on in order for a fixture to illuminate. Fixtures in the preexisting system contain 8 watt F8T5CW bulbs capable of outputting 340 lumens of light [11]. Due to losses in the lighting ballast the actual power consumption was measured to be 9.24 watts per fixture making total system power consumption 55.44 watts. When used with 3 LEDs in series the Macroblock MBI6651 features an efficiency of 96% [9] making the power consumption of each module 3.125 watts and total system consumption 18.75 watts when 6 modules are used. Other added benefits include networkability and the ability to dim LED lights which cannot be done with most fluorescent lighting systems. Dimmer control is completed through a potentiometer featured in the right hand side of the dashboard. The potentiometer itself is

connected to the input module through an 8 bit analog to digital converter which outputs a digital value between 0 and 255 corresponding to the duty level of the interior lighting system between 0% and 100% respectively. Since each light module is capable of being networked and activated via the CAN bus the system can easily be expanded to different numbers of modules. The only connections necessary for additional modules are a 12 volt DC power source and the ability to connect to the CAN bus network. Smart functions can also be programmed to trigger the lights on or off using other sensors and inputs of the control system. A great example would be turning the interior lights on and off based on the state of the door position. Rather than requiring additional sensors and circuitry, a function like this can simply be added through additional program code. Superior performance is also seen in the form of reduced maintenance. Each of the 1 watt LEDs used in this system are rated for 50,000 [10] hours of use which far exceeds the 7500 hour [11] lifespan of fluorescent bulbs used in the preexisting system.

4.0 Headlights and Accessories Load Module

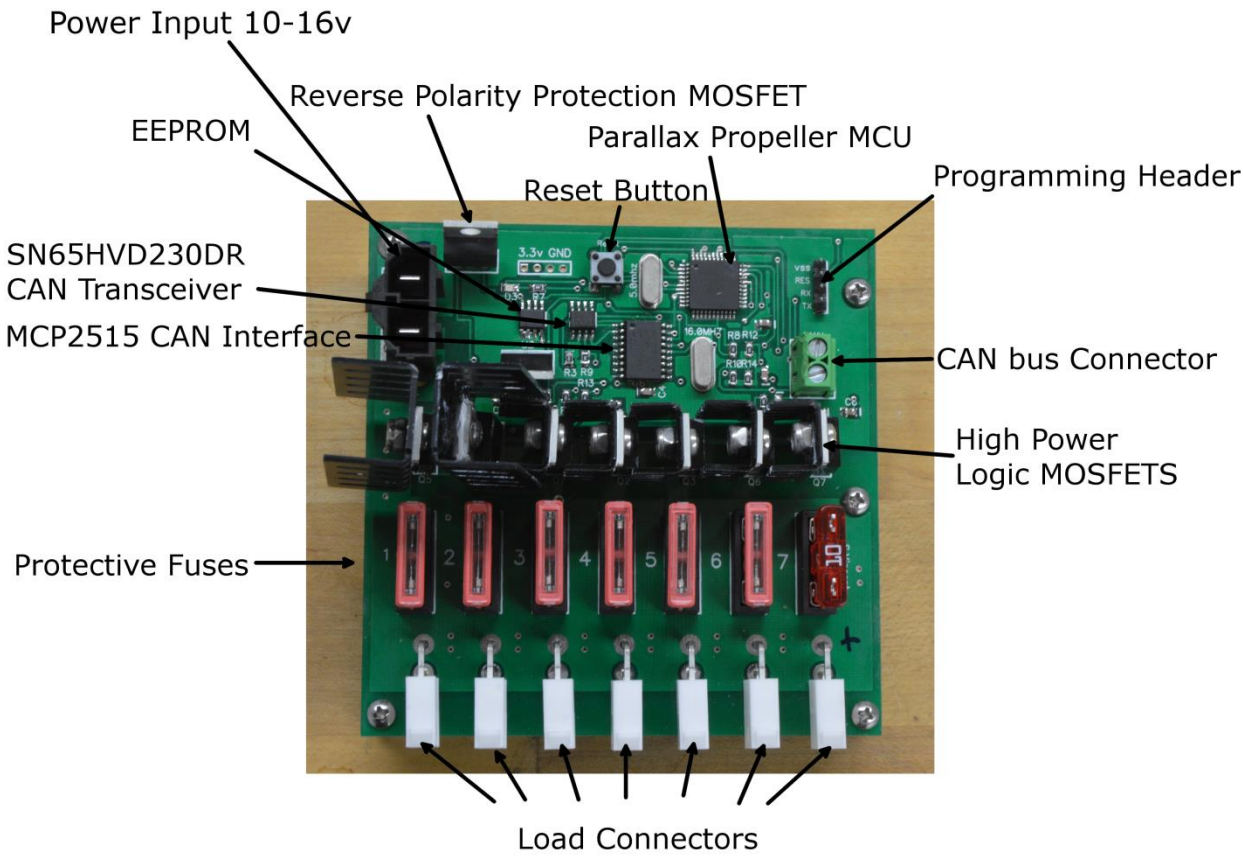

Figure 4.1: Headlights and Accessories Module

4.1 Headlights and Accessories Module Overview

Electric vehicles require a number of auxiliary features both for convenience and in order to meet legal driving requirements. Front exterior lighting and accessories are controlled by two Headlights and Accessories Load modules (Fig. 4.1) located in the front panel of the bus. An additional module, located in the rear of the bus, controls the rear exterior lights. All of the modules feature CAN bus network connectivity allowing easy interaction between modules with only a single twisted pair connection. Network connectivity between modules also allows for smart feature creation based on any of the other sensor or manual inputs in the system. For example, with networked modules it is possible to program the warning flashers to turn on when

the door is open or for the door to automatically close once a certain speed has been attained. Each module is capable of switching up to 7 loads using high powered logic MOSFETS.

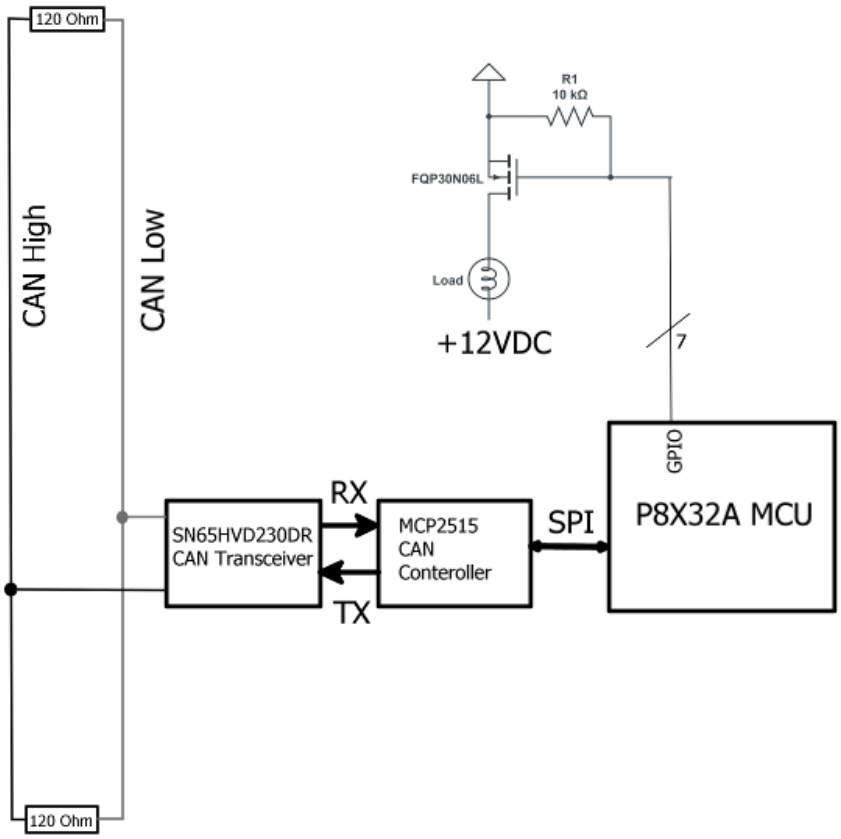

Figure 4.2: Headlights and Accessories Module Flowchart

4.2 Comparison with Preexisting Load Switching System

The previous system installed in the University of Kansas' electric bus featured an entirely analog system using twelve volt automotive relays for all load switching. This system requires either a separate switch to be wired in parallel for each different function or an entirely separate circuit. For example, warning flashers typically use the same lights used by the turn

signals. In an entirely analog system either two different switches would be need to be wired in parallel for each bulb as shown in figure 4.3.

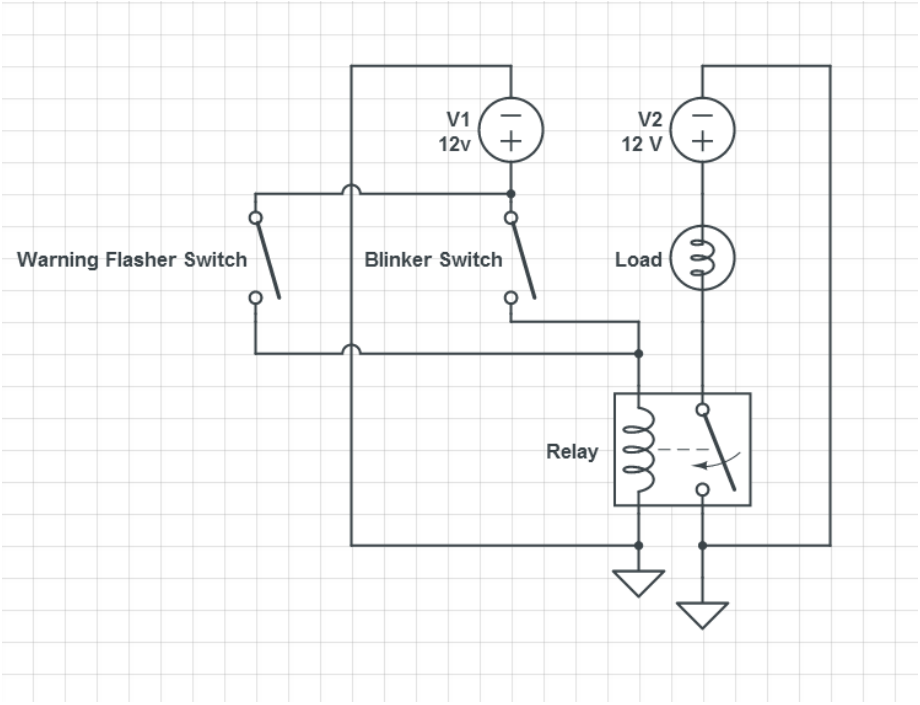

Figure 4.3: Relay based Turn Signal/Warning Flasher Example Wiring #1

Or they can be wired using two completely separate relay circuits, one for the hazard lights and the other for the turn signal as shown in Figure 4.4

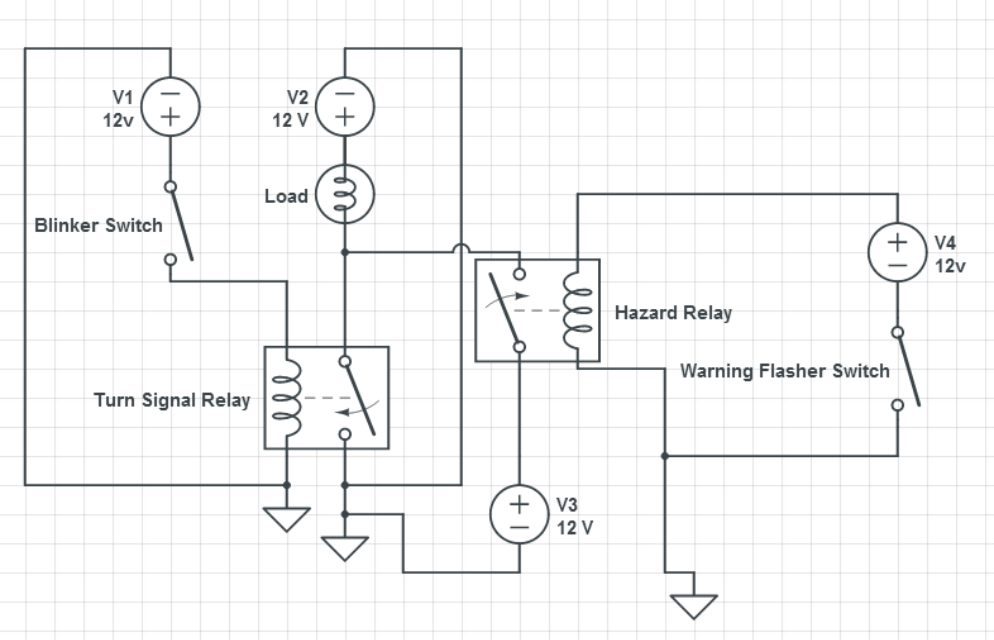

Figure 4.4: Relay based Turn Signal/Warning Flasher Example Wiring #2

Either configuration can result in a large number of additional components and complex wiring, particularly when coordinating functions at opposite ends of the vehicle such as front and rear lighting applications. The University of Kansas's electric bus used multiple relays and separate circuits for each function similar to Figure 4.4. As can be seen in Figure 4.5 this results in a sizable system with copious amounts of wiring.

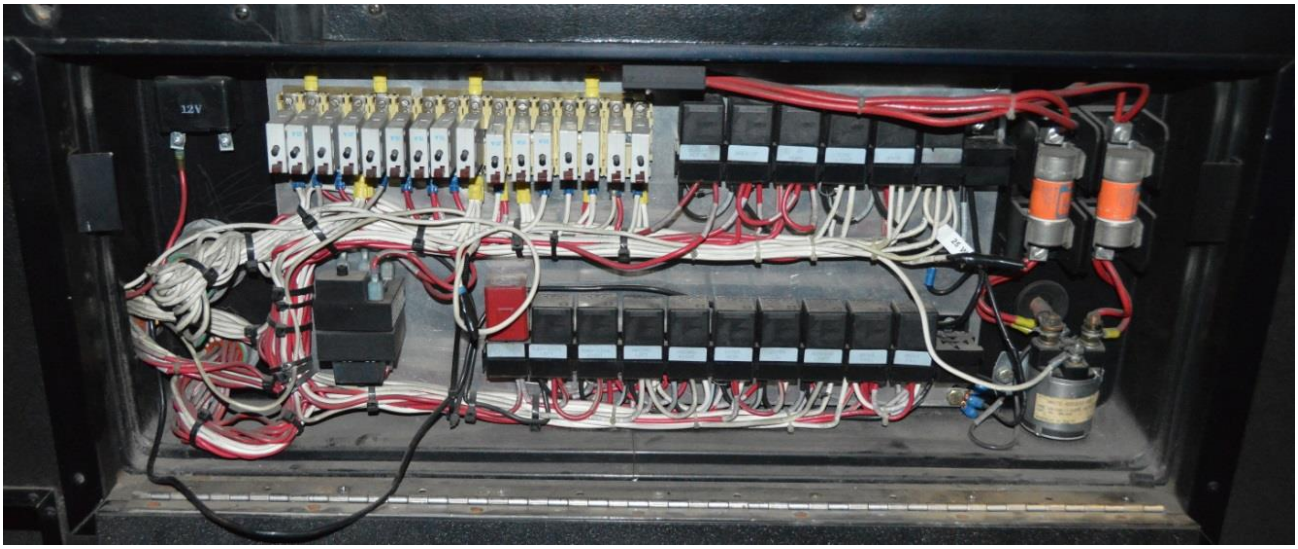

Figure 4.5: Preexisting Relay Based System

Wiring complexity makes both installation and system troubleshooting difficult.

4.3 Headlights and Accessories Module System Architecture

Digital load control using programmable microcontrollers allows for much simpler wiring with only one circuit connected to each load. Additional functions can easily be added through changes in program code without any need for changes in circuitry.

Logic MOSFETs were chosen for many reasons including their greatly increased lifespan, high speed switching capabilities, small size and high efficiency.

Automotive relays typically have a life-cycle expectancy somewhere in the range of 100,000 cycles at their full rated load [12]. Increased temperatures due to high cycle rates and a warm environment can also work to reduce the lifespan of a mechanical relay [13]. On the other hand Logic MOSFETS are capable of millions of cycles before failure.

Logic MOSFETS are capable of switching at very high speeds due to delay and rise times on the order of nanoseconds [14]. High speed switching allows MOSFETS to be used to pulse width modulate the power input of items such as motors or lights and thus vary the corresponding power output. The ability to vary loads based on demand is often much more efficient than running at a single load level with a relay due to the dynamic nature of most systems. The ability to pulse width modulate the output of a MOSFET makes them much more versatile than relays which only offer on-off operation.

Another benefit of using MOSFETs for load switching is a decrease in size. Figure 4.6 shows that even when fit with a large heatsink necessary for switching larger loads, a MOSFET is much smaller than a common automotive relay.

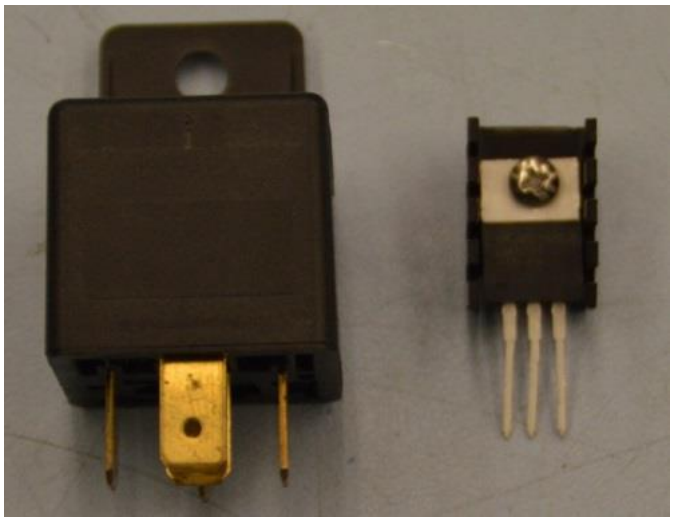

Figure 4.6: Relay vs TO-220 Package MOSFET size comparison

Unlike bipolar junction transistors which require a gate current to turn on and off, N-Channel logic MOSFETS only require a voltage. This means that once the gate is charged to 3.3 V current flow is near zero, requiring very little power from the microcontroller. As a result a

pull-down resistor must be used to allow the gate to quickly discharge preventing floating as seen in figure 4.7.

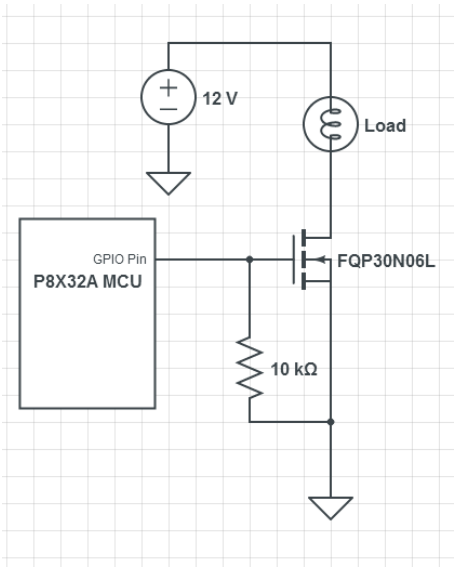

Figure 4.7: Low Side MOSFET Load Control Schematic

As seen in Figure 4.7 all MOSFETS are controlled from the low side. This means that the load has been placed between the positive voltage source and the drain. In order to drive a MOSFET from the high side, where the load is placed between the source and ground the voltage between the gate and source must be higher than that of the voltage between the voltage between the drain and source. This requires additional components to raise the voltage of the input pin in the case of a high side configuration.

4.4 Proposed System Layout

When switching a MOSFET activated by a microcontroller, many different functions can be applied to each load while maintaining the same simple wiring. Coordination between items on opposite ends of the bus is also made simpler by simply placing several headlight and accessories modules in the front of the bus and one in the back of the bus. The only wiring

necessary in this configuration is a power connection in the front and back of the bus and then a single twisted pair connecting all of the modules in the bus together via CAN bus. This also makes the system easily expandable as the number of Headlight and Accessories modules can easily be changed to suit different applications. Three Headlight and Accessories modules will be used in this particular application. In each case inputs are gathered from the input modules and then sent over the CAN bus via different CAN ids and locations in the CAN buffer. The following three tables, (tables 4.1-4.x) show the input-output mapping for each particular function on the three different modules used.

Front Module 1

Output Description	Output #	Input CAN ID	CAN Buffer Location	Input Type	Input Range	Active Range
Left Blinker	1	$000	canbuf[0]	Digital	0-1	1
Wiper 1 Low	2	$002	canbuf[3]	Analog	0-255	91-159
Wiper 1 High	3	$002	canbuf[3]	Analog	0-255	160-250
Washer Fluid	4	$002	canbuf[3]	Analog	0-255	250-255
Right Blinker	5	$000	canbuf[1]	Digital	0-1	1
Left Headlight	6	$000	canbuf[4]	Digital	0-1	1
Right Headlight	7	$000	canbuf[5]	Digital	0-1	1
Warning Flashers	1,5	$000	canbuf[2]	Digital	0-1	1

Table 4.1: Front Module 1 Input/Output Mapping

Front Module 2

Output Description	Output #	Input CAN ID	CAN Buffer Location	Input Type	Input Range	Active Range
Stop Indicator	1	$000	canbuf[6]	Digital	0-1	1
Door Open	2	$000	canbuf[7]	Digital	0-1	1
Wiper 1 Low	3	$002	canbuf[3]	Analog	0-255	91-159
Wiper 1 High	4	$002	canbuf[3]	Analog	0-255	160-250
open	5					
open	6					
open	7					

Table 4.2: Front Module 2 Input/Output Mapping

Rear Module 1

Output Description	Output #	Input CAN ID	CAN Buffer Location	Input Type	Input Range	Active Range
Left Blinker	1	$000	canbuf[0]	Digital	0-1	1
Open	2					
Open	3					
Open	4					
Right Blinker	5	$000	canbuf[1]	Digital	0-1	1
Open	6					
Open	7					
Warning Flashers	1,5	$000	canbuf[2]	Digital	0-1	1

Table 4.3: Rear Module 1 Input/Output Mapping

4.5 Headlights and Accessories Module Efficiency Considerations

An equivalent relay based switching system would require the use of many additional components as well as greater power usage. Automotive relays commonly require around 1.8 watts in order to maintain their switched state. This means a system comparable to the Headlight and Accessories module would require 12.6 watts solely for the purpose of maintaining a switched on or high state. A majority of microcontrollers feature GPIO pins with 3.3 V or 5.0 V logic and thus an additional Bipolar Junction Transistor is typically used to switch a 12 V source through the relay's coil. In this type of setup a small amount of current must be sent to each BJT in order to maintain a desired state. The FQP30N06L Logic N-Channel MOSFETs used have an *Rds* resistance of only .035Ω [14]. As a result the i^2R losses from running the highest current load on the electric bus, a 55 watt headlamp, which settles to a constant current draw of 3.4

Amps is only 0.405 watts. Since MOSFET $i^2 R$ losses reduce greatly when considering lower current loads the losses from other loads are significantly less.

4.6 Load Types

Headlights and accessories modules interface with a number of different loads, most of which require only a simple on-off control. This is also the case interfacing with the air powered door, which simply requires 12 volts to be sent to an exhaust type solenoid valve as seen in figure 4.8 resulting in door actuation.

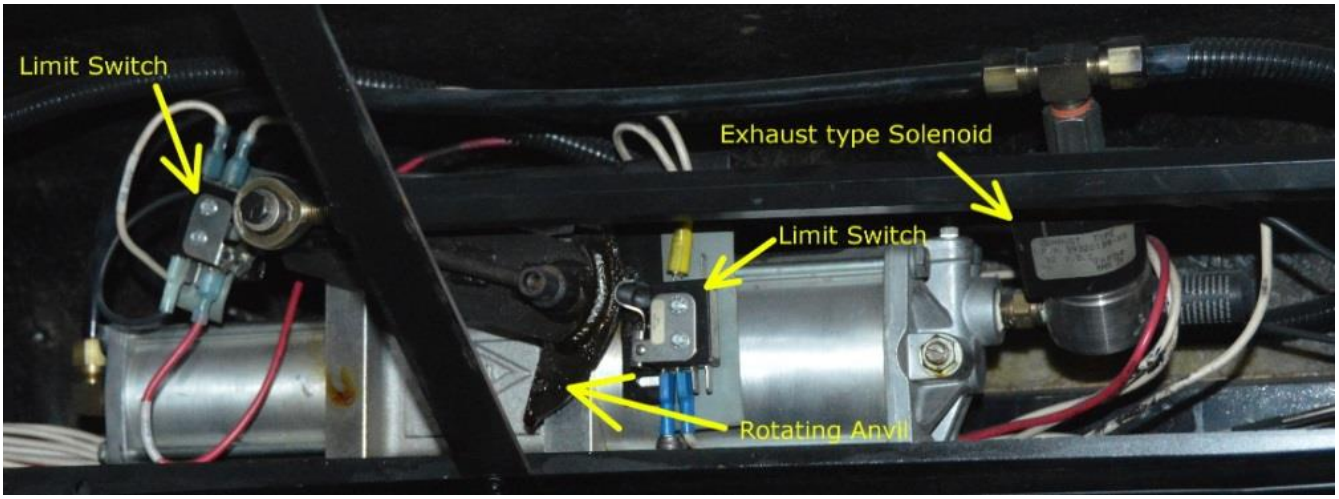

Figure 4.8: Pneumatic Door Control Implementation

Limit switches, seen in figure 4.8, built into the door modulate the exhaust type solenoid valve on and off once the door hits its full open or closed position. Due to the existing analog circuits ability to modulate airflow based on the rotating anvil swinging and depressing limit switches at the fully opened and fully closed position the bus only need to connect to the power leads connected to the relay from the preexisting control system.

Windshield wiper motors have a slightly different interface due to the motors ability to run at multiple speeds coupled with a park position. Though most DC motors can be speed controlled via pulse width modulation using only one MOSFET, this system was designed to interface with standard automotive components. In the case of common wiper motors speed control is completed by varying which connection point 12 V is fed to.

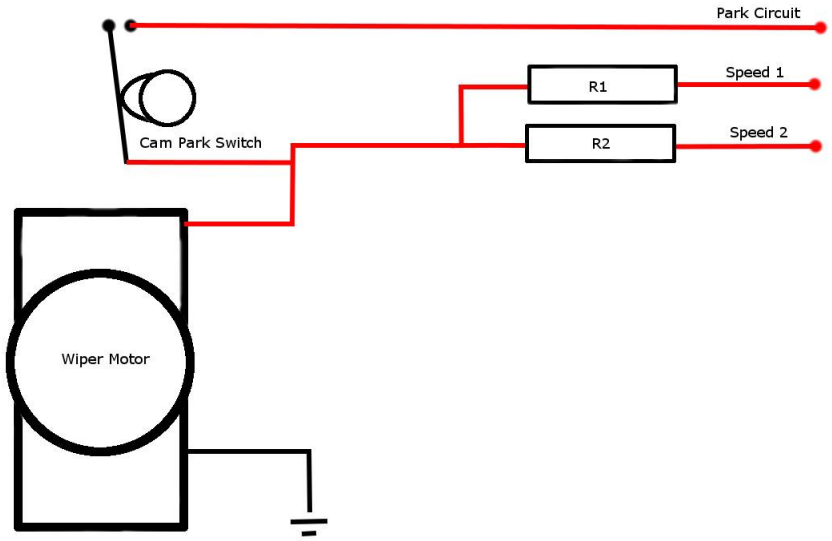

Figure 4.9: Two-Speed Wiper Motor Control Schematic

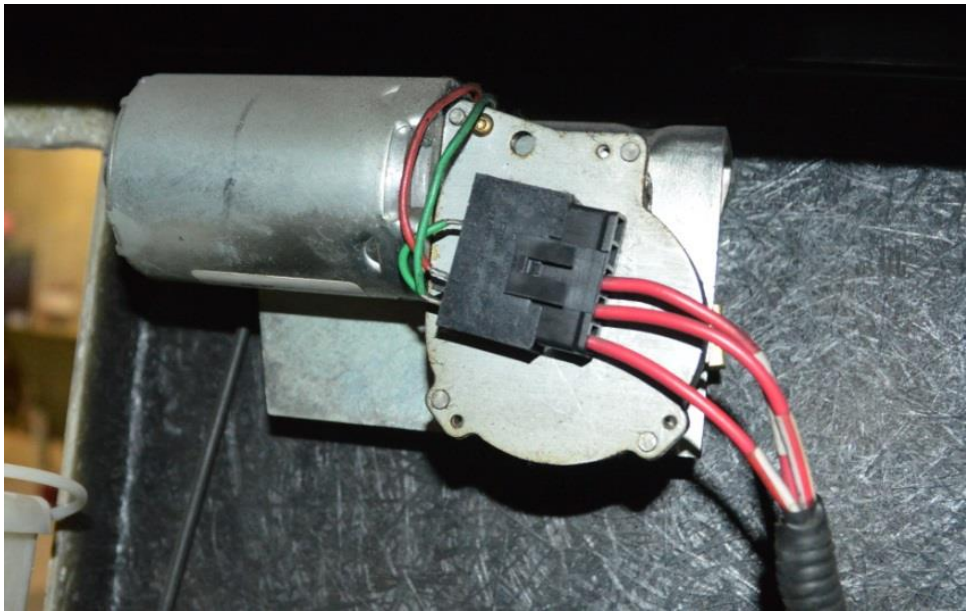

Figure 4.10: Electric Bus Wiper Motor

As is seen in Figures 4.9 and 4.10 the University of Kansas electric bus has wiper motors with two speeds, in this case the connection for each speed has a different resistance varying the current through the motor. Speed selection is accomplished by controlling which of those two input leads receives a positive 12 volts. In addition to both speed inputs a third input is hooked directly to a positive 12 volt source to run the wiper's park function. This function returns the wiper to a rest position when they are turned off in any other position. This is completed by a cam shaped switch creating a circuit to run the motor anytime it is not in the home position. When in the home position the cam switch opens the park circuit requiring that one of the MOSFET switched power inputs be on in order to move the motor. The University of Kansas electric vehicle has two independent wiper motors each with its own park function requiring the use of four switched positive 12 volt sources from the Headlight and Accessories module.

5.0 Accelerator Pedal Sensor Module

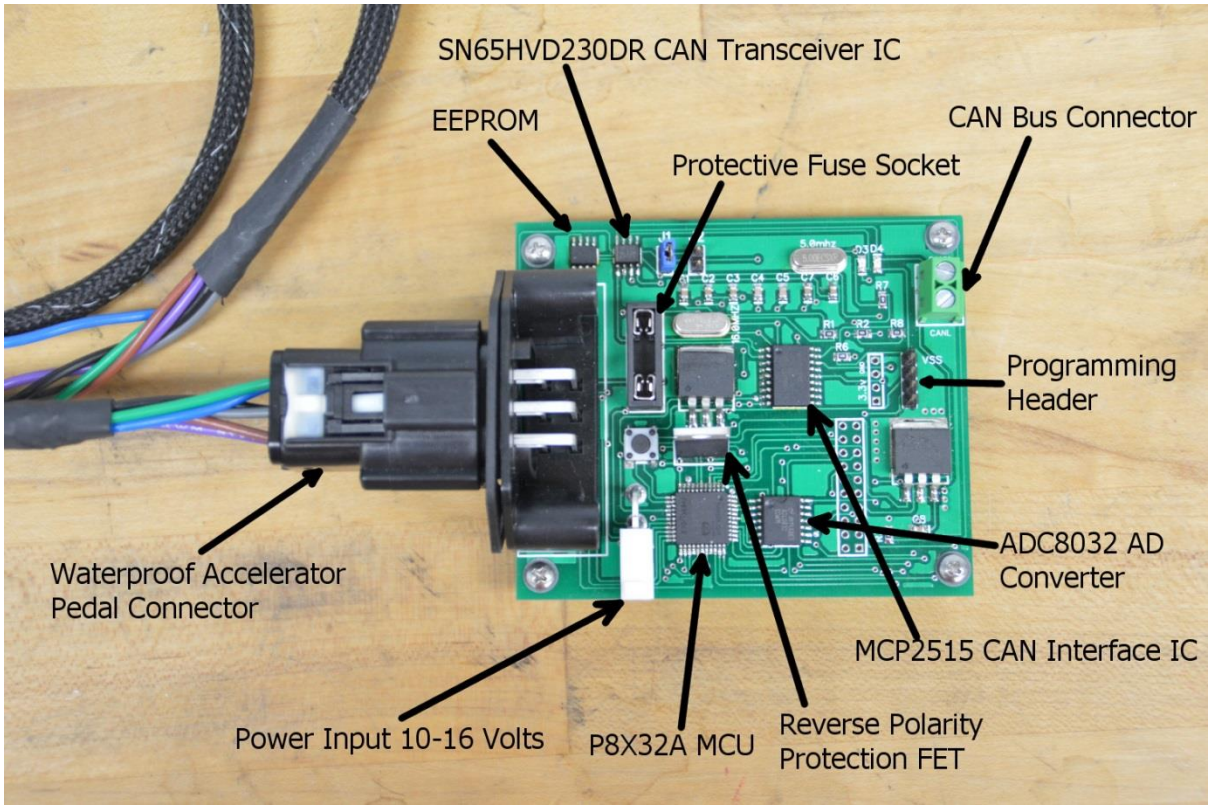

Figure 5.1: Accelerator Pedal Sensor Module

5.1 Accelerator Pedal Sensor Module Overview

The purpose of the Accelerator pedal module is to read accelerator pedal position data from two redundant sensors and send that data to the rest of the bus control system via the CAN bus network. This module was made separately from any other functions so that when coupled with motor controllers using CAN inputs for speed data, the module could be hooked either directly to the motor controller or through an existing CAN network.

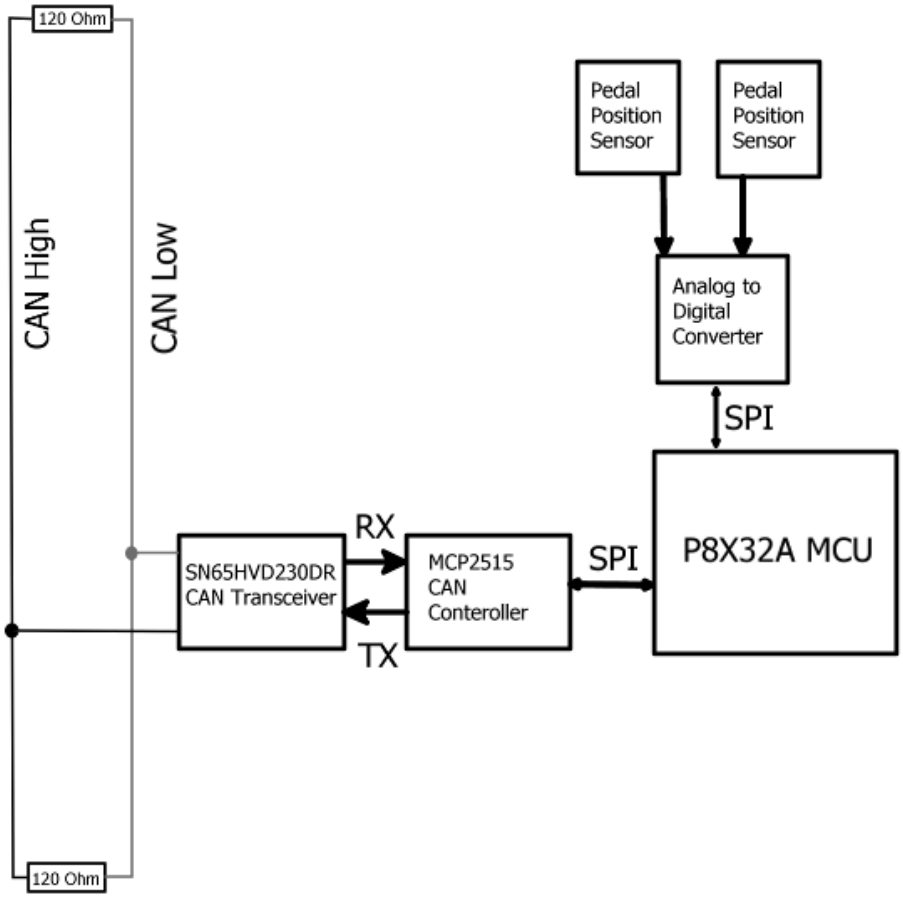

Figure 5.2: Accelerator Pedal Module Flowchart

This module was also produced separately in an effort to minimize electrical noise and possible sources of failure and error. Additionally, this system was designed to work with common drive by wire accelerator pedals and sensors and uses a similar system of checking redundant sensors as an effort to prevent unwanted acceleration or deceleration. Due to the design and ability to upload different program code this module is capable of working with the existing accelerator pedal or standard drive by wire pedals in the event of an upgrade.

5.2 Drive by Wire System Background

Drive by wire systems were first introduced into the market in the late 1990's and early 2000's in gasoline powered luxury cars produced by Audi, Mercedes-Benz, Lexus, and BMW [21]. These systems are now commonly featured on gasoline powered vehicles rather than cable driven systems due to their ease of installation, reliability, improved response time, and added features. Drive by wire systems read the input of an accelerator pedal position sensor, or multiple sensors, and then pass that information on to a microcontroller where the data is used to vary the vehicle's speed. Typical drive by wire accelerator pedal systems feature a mechanical assembly containing a pedal and linkages required to rotate an accelerator position sensor as pictured in figure 5.3.

Figure 5.3: Lokar Drive by Wire accelerator Assembly [16]

5.3 Accelerator Pedal Sensor Module System Architecture

Accelerator position sensing is typically done with redundant potentiometers sending a value to a microprocessor where the analog input of each is converted into a digital value [17]. Older systems relied on mechanical potentiometers, while newer systems often use more reliable hall-effect based sensors.

5.3.1Circuit

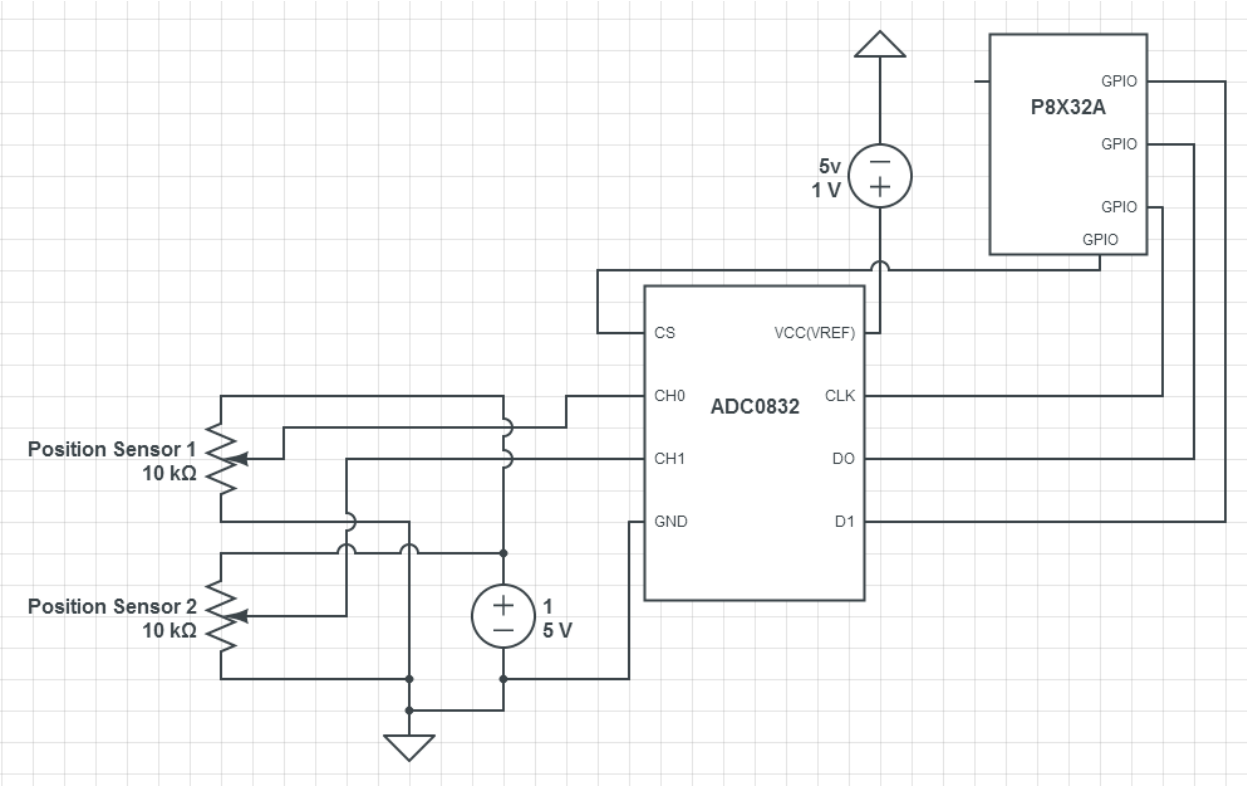

Figure 5.4: Analog to Digital conversion circuit

This module uses the ADC0832 Analog to digital converter IC made by Texas Instruments. Figure 5.4 shows how the chip is wired into the parallax propeller microcontroller unit. This chip features an eight bit resolution along with the ability to read from two different inputs making it an excellent choice for reading redundant position sensors from a drive by wire accelerator pedal

5.4 Redundancy based fault checking

Many different methods of fault checking exist, however redundancy based checking methods are capable of detecting faults faster and with higher precision [18]. Redundancy based methods generally work by reading signals from two sensors placed on the same input, finding the difference between those signals and checking whether or not that discrepancy is within a predetermined tolerance value. In the case of fault detection, this system is programmed to immediately change the motor output to zero and send a message to the CAN bus signaling a fault. This message will be displayed on the 16x2 LCD placed in dashboard.

6.0 Battery Voltage Sensor Module

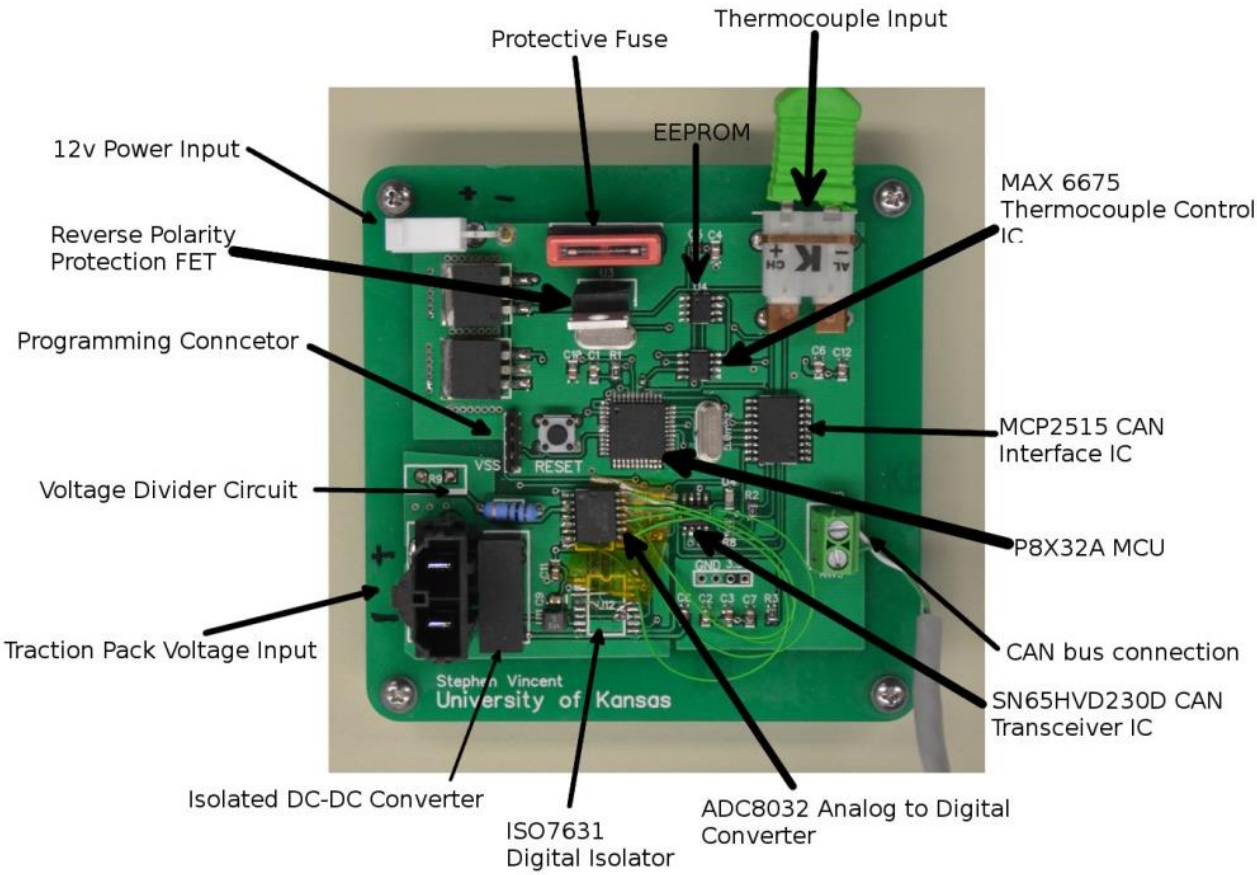

Figure 6.1: Battery Voltage Sensor Module

6.1 Battery Voltage Sensor Module Overview

Battery voltage is read by the battery voltage module Fig 6.1 and sent over the CAN bus network to the speed sensor and display module where it is displayed on the 16x2 character LCD. This task is completed by using an isolated analog to digital converter to read $1/100^{th}$ of the electric vehicle's battery pack voltage (also known as the traction pack voltage). An additional feature of the battery voltage sensor module is temperature monitoring capabilities via a type K thermocouple. This feature was included in this module due to the battery packs proximity to the motor inverter which will have its temperature constantly monitored to prevent damage.

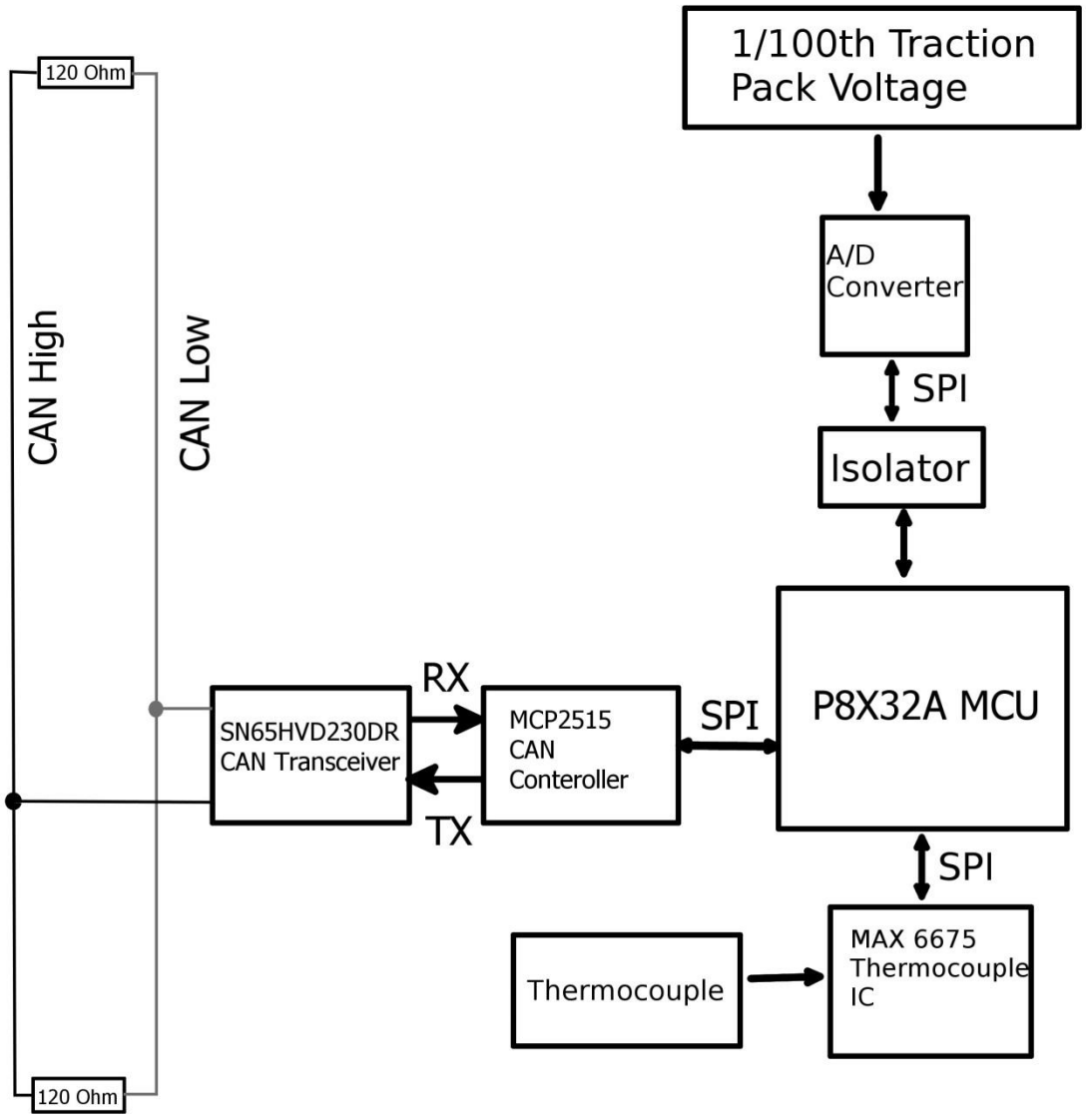

Figure 6.2: Battery Voltage Sensor Module Flowchart

It is important to know the current traction battery pack voltage when driving electric vehicles to prevent stranding the vehicle away from a charging station. This task is often difficult due to the high voltage of the battery pack itself. In the case of the University of Kansas electric bus the nominal voltage of a fully charged traction battery pack is 414 volts. The battery

voltage sensor module is designed to handle voltages as high as 500 volts providing a margin of safety in the event of an overcharged pack or upgrade to a higher voltage battery system.

6.2 Battery Voltage Sensor Module Architecture

Battery voltage is measured using an ADC8031 analog to digital converter [19] with a 5v reference voltage. Due to the battery packs much higher voltage it is first run through a voltage divider circuit with a high power resistor to bring the voltage down to 1/100th of the actual pack voltage. Using the common voltage divider circuit shown in figure 6.3 with R1=10MΩ and R2= 100kΩ the output voltage is given by the following equation $V_{out} = \frac{R2}{R1+R2} * V_{in}$ where $V_{in} = Traction\ pack\ voltage.$

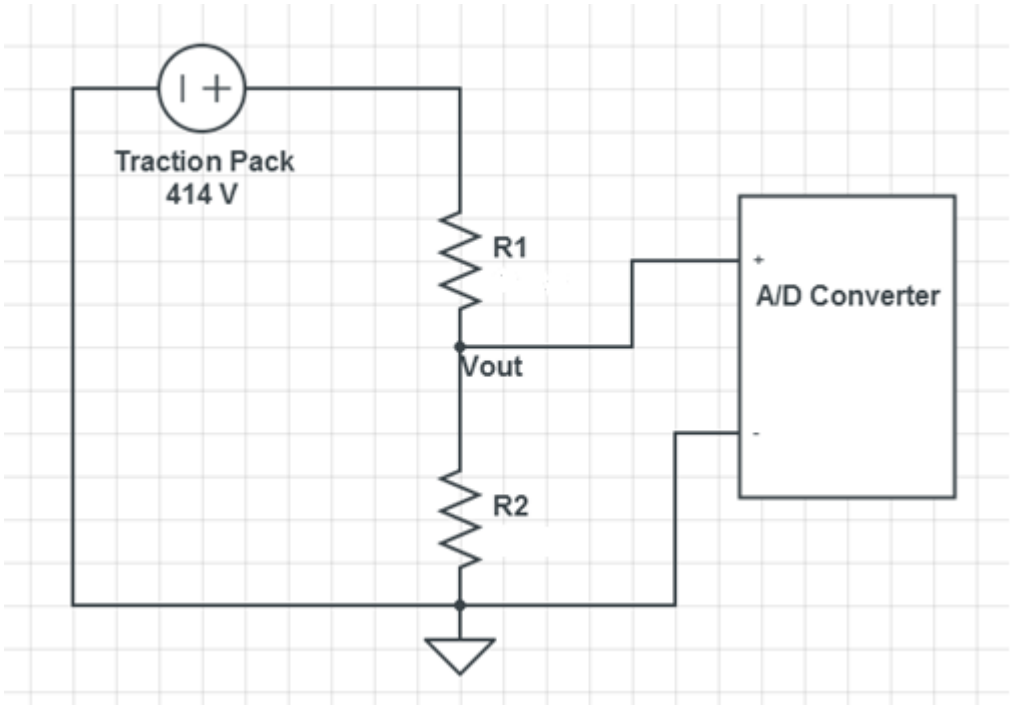

Figure 6.3: Voltage Divider Schematic

This yields a V_out ranging from 4.95 v at the maximum of 500v making it compatible with the ADC8031 analog to digital conversion chip. The resolution of analog to digital conversion, *Q*, is given by equation 6.1

$$Q = \frac{E_{fsr}}{2^{M}-1} \quad \text{(Eq. 6.1)}$$

where E_{fsr} is the full scale voltage and M is the number of digital bits of resolution offered by the analog to digital conversion chip. In this case the resolution is $\frac{500v}{2^{8}-1}$ or 1.96v. This is more than adequate resolution as the module itself is only needed to give a rough idea of the current voltage state and is not being used to control any other systems.

Careful consideration must be taken when using a voltage divider circuit with high voltage systems due to the large amount of heat dissipated by the power resistor R1 in figure 6.3. Using ohms law, $V = IR$,where I is current in amps and *R* is resistance in ohms we can solve to find that the maximum current through the circuit is $.0495\ ma = 500v/10.1Mohms$. Power dissipation in the resistors is given by the following equation $P = I\text{^}2R$ where *P* is power dissipated in watts, *I* is the current through the resistor in amps and *R* is the resistance in ohms. In this case the larger resistor dissipates .0245 watts at 500v and .016 watts at 414v. If lower resistance values yielding the same Vout power dissipated in the resistor will be much higher resulting in the possibility of overheating.

Due to the high voltage of the battery pack being measured, the analog to digital converter has been digitally isolated from the rest of the circuit to prevent possible module damage caused by ground loops. This was accomplished using a Texas Instruments ISO7631

low power triple channel digital isolator [20] powered by a Murata MEV3S0505SC isolated 5v power supply [21].

Temperature monitoring functions are completed via a MAX6675 [22] thermocouple IC and type K thermocouple. This particular IC was chosen due to its 12bit, 0.25 degrees C resolution and ease of interfacing with a microcontroller using the Serial Peripheral Interface protocol. Additionally, the MAX6675 is designed for use in harsh automotive environments and has an operating temperature range of -20 degrees C to +85 degrees C [22].

7.0 Input Module

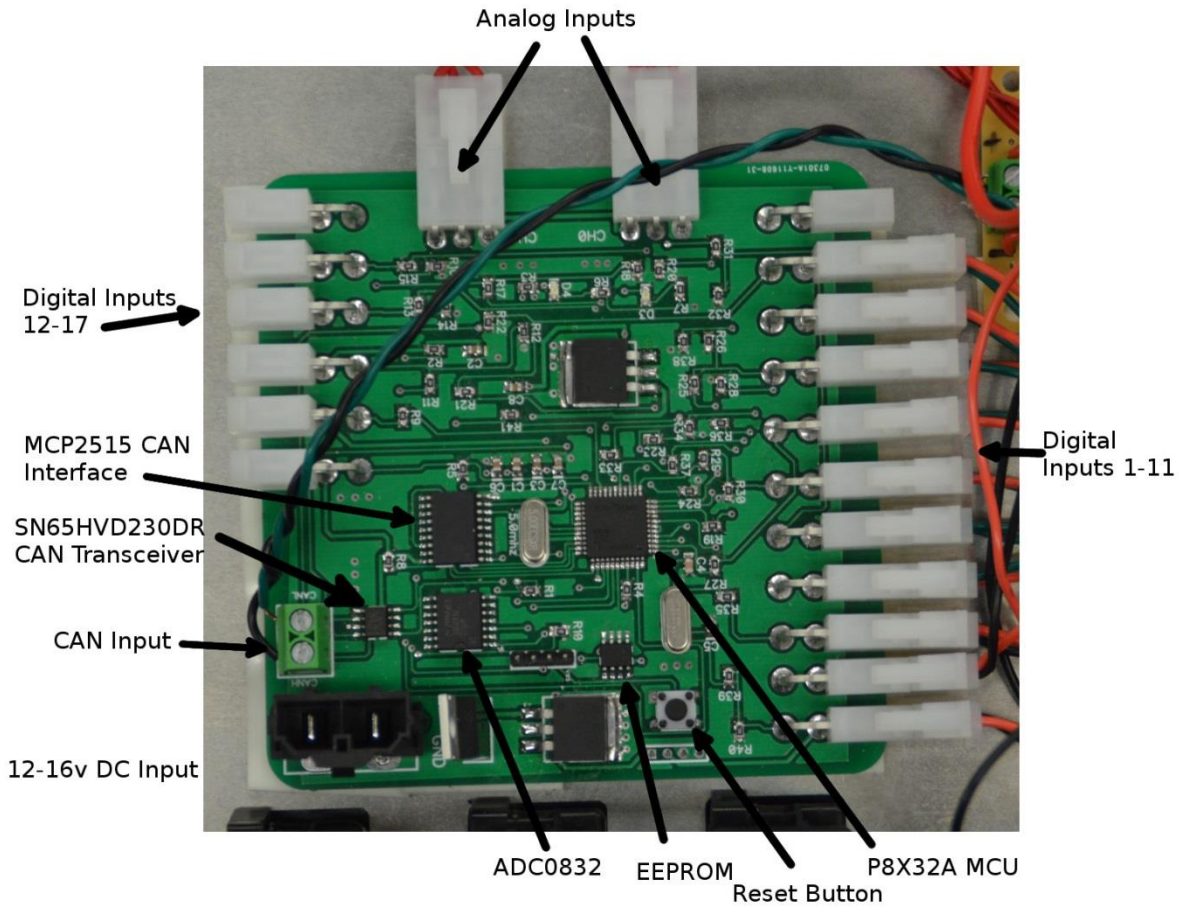

Figure 7.1: Input Module

7.1 Input Module Overview

The purpose of the input module is to read user inputs, process them and transmit the input states over the CAN bus. Input state information is pulled off of the CAN bus by the three headlight and accessories modules as well as an interior lighting module. Attached loads are controlled in various ways according to program code. For most loads control is completed by simply providing the device with 12 V. The input module is capable of reading digital input for simple on/off functions as well as reading analog inputs for items with variable speed such as windshield wipers. In the preexisting analog system on this electric bus each input was completed with a simple on/off switch included as part of each circuit. A networked system allows multiple inputs to affect one output without complex wiring. Additionally, wiring is reduced greatly because the only connection needed between inputs and outputs is a twisted pair terminated on either end with 120 ohm resistors for the CAN bus network. The input module is connected to the CAN bus and reads inputs as seen in the flowchart in figure 7.2.

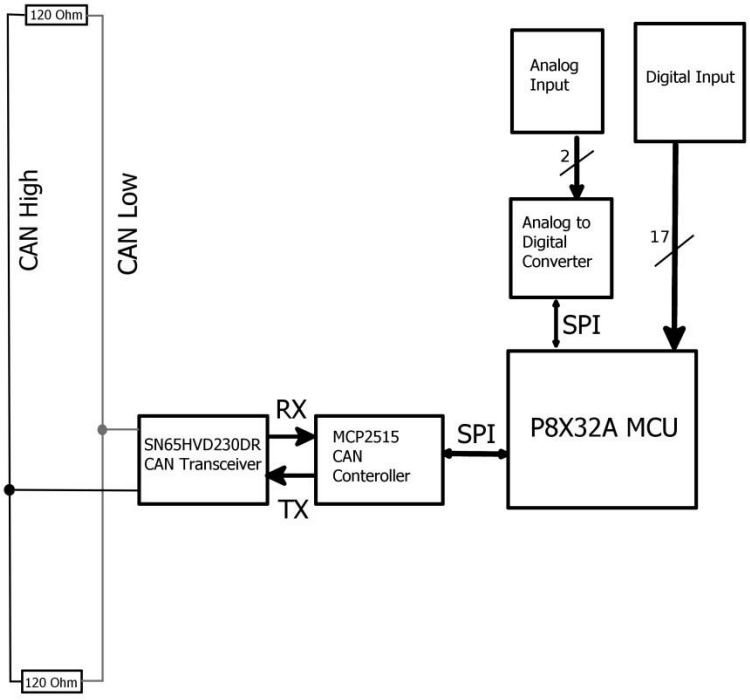

Figure 7.2: Input Module Flowchart

7.2 Input Module System Layout and Architecture

The preexisting system resulted in a large dash panel cluttered with switches as seen in figure 7.3.

Figure 7.3: Preexisting Dashboard Controls

This is due to the fact that nearly every function needs a separate switch and the switches used have a fairly large footprint. This also results in a cumbersome user experience for most drivers since it operates very differently than a standard passenger car. In an effort to make the control system function more like a passenger car, the input module was designed to interface with a standard car multi-function switch as seen in figure 7.4.

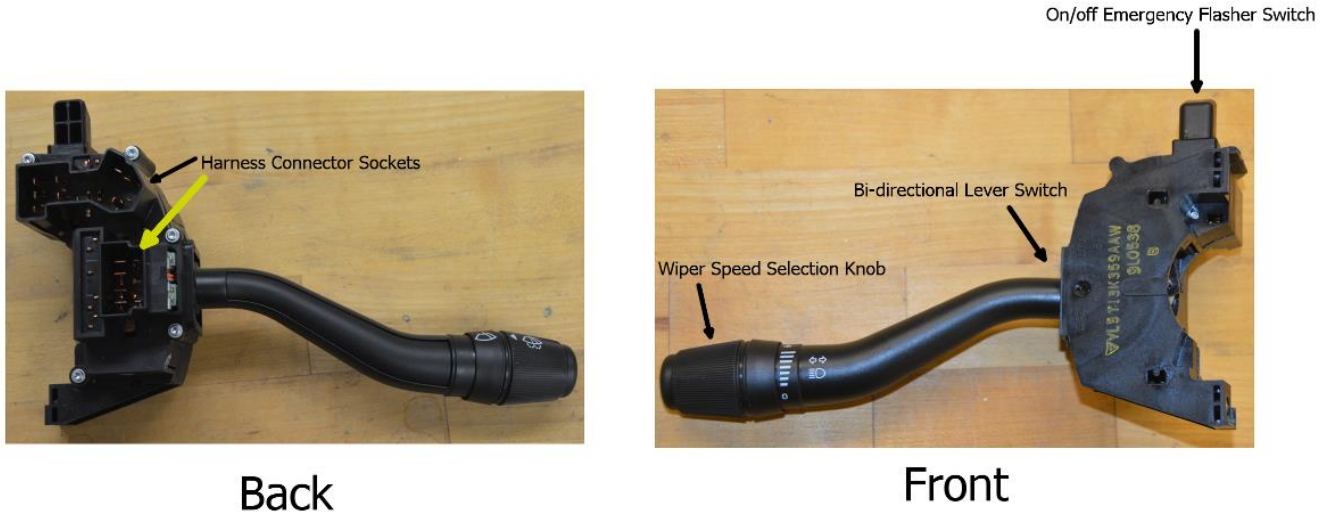

Figure 7.4: Multifunction Switch

Turn signals, emergency flashers, windshield wipers, and washer fluid spray activation are all controlled using the multifunction switch pictured in figure 7.4. Turn signals are activated by tilting the bi-directional lever switch counter-clockwise for the left turn signal and clockwise for the right turn signal. Warning flashers are turned on and off by pushing in on the switch labeled on/off emergency flasher switch in Figure 7.4. Windshield wiper motors are activated by turning the knob labeled Wiper Speed Selection Knob in figure 7.4 counter clockwise. Turning the knob varies a resistor resulting in a varying analog input to the module. Washer fluid spraying is

activated by pressing inward on the wiper speed selection knob causing an open circuit. As a result of the multifunction switch taking the place of multiple different functions the new dashboard system will be more organized and intuitive for users. A test setup was built for display purposes and can be seen in figure 7.5.

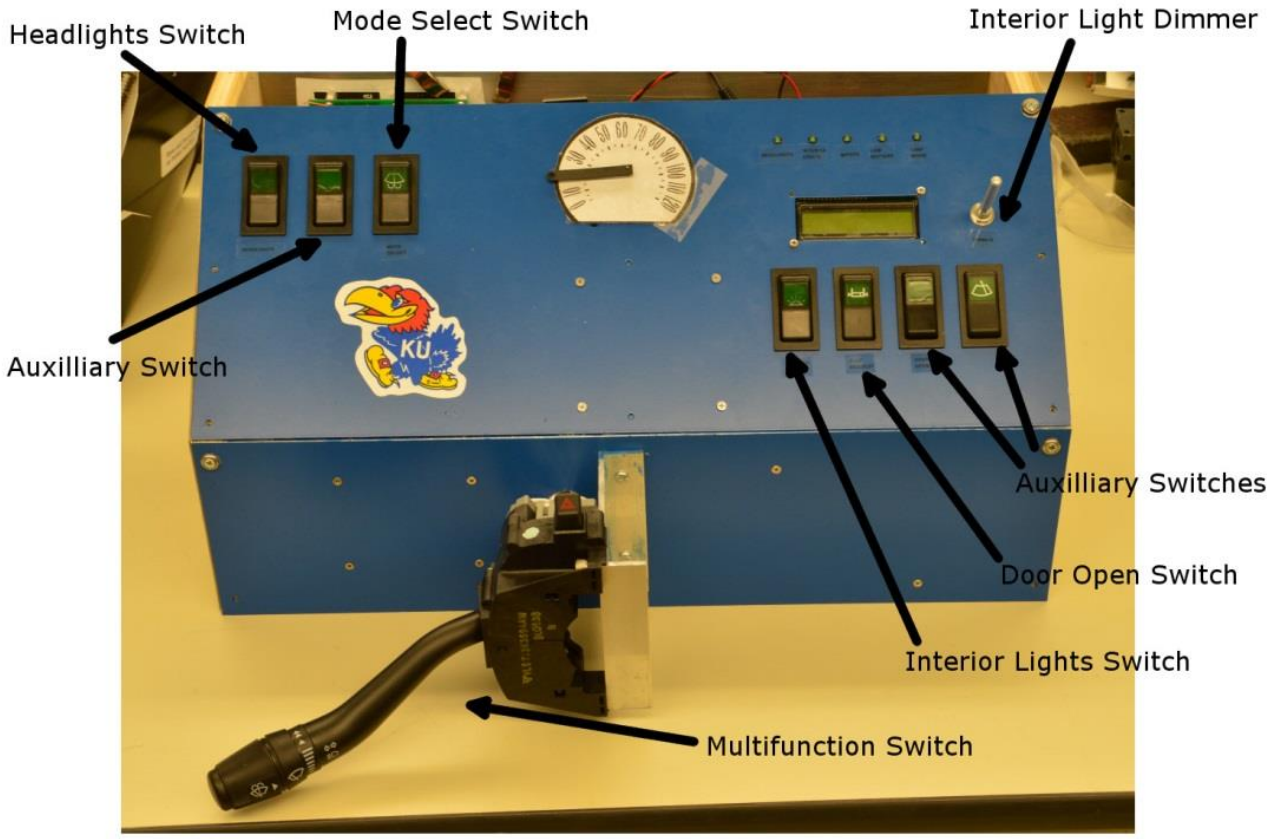

Figure 7.5: Demonstration Dashboard

The input module is designed to handle all of the user inputs for bus control system. Exceptions to this rule are the accelerator pedal which was made into a separate module to reduce the possibility of failure and the brakes which are an entirely mechanical system. Nine

digital inputs and 2 analog inputs are controlled via the input module which can be seen in table 7.1.

Function (output)	Input Type	CAN ID
Left Turn Signal	Digital	$000
Right Turn Signal	Digital	$000
Warning Flasher	Digital	$000
Headlights High Beam	Digital	$000
Headlights Low Beam	Digital	$000
Door	digital	$000
Stop Request Sign	digital	$000
Washer Fluid spray	digital	$002
Forward/Reverse	Digital	$002
Interior Lights On/Off	Digital	$001
Interior Lights Dimmer	Analog	$002
Wiper (variable speed)	Analog	$002

Table 7.1: User Input Mapping

Due to the low cost and ease of adding additional inputs to the input module, extra digital inputs were added to account for future system expansion. If a number of inputs beyond what one input module will handle is required a second input module could easily be incorporated into the system with a simple connection to the CAN bus twisted pair. In total the system will have 17 digital inputs and 2 analog inputs. Digital inputs will be connected to GPIO pins of the P8X32A MCU and a 10k pull down resistor to prevent logic levels from floating. Digital inputs will be connected to a 3.3 V source through different types of switches and then run through a 1k resistor to limit the current to each input pin to 3.3 ma. Figure 7.6 shows the schematic for a digital input as is used in this system.

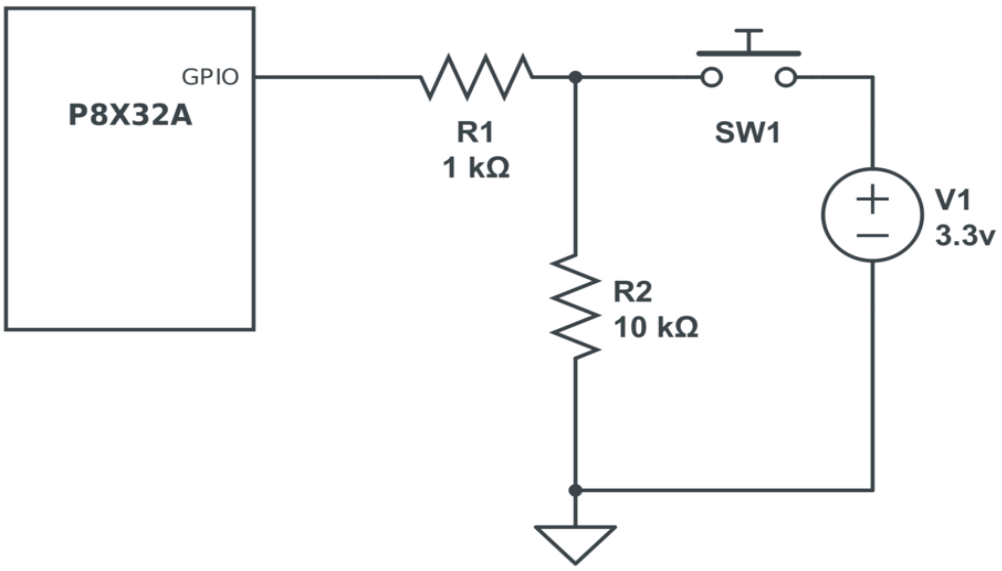

Figure 7.6: Digital Input Schematic

Analog inputs are connected to the system using a two-channel, eight bit ADC0832 analog to digital conversion IC [19]. The ADC0832 chip is powered by a 5v supply and will also use 5v as a reference supply. Since this is an 8 bit analog to digital conversion chip the IC will return a value between 0 and 255 for each channel. The resolution is given by the taking the reference voltage and dividing it by the maximum number output number yielding $\frac{5volts}{255} = .0196\ volts.$ Therefore the measured voltage will be equal to the resolution multiplied by the analog to digital converters output. Each channel of the analog to digital converter will be hooked up as shown in figure 7.7 only the chip used will have inputs for four different analog sources.

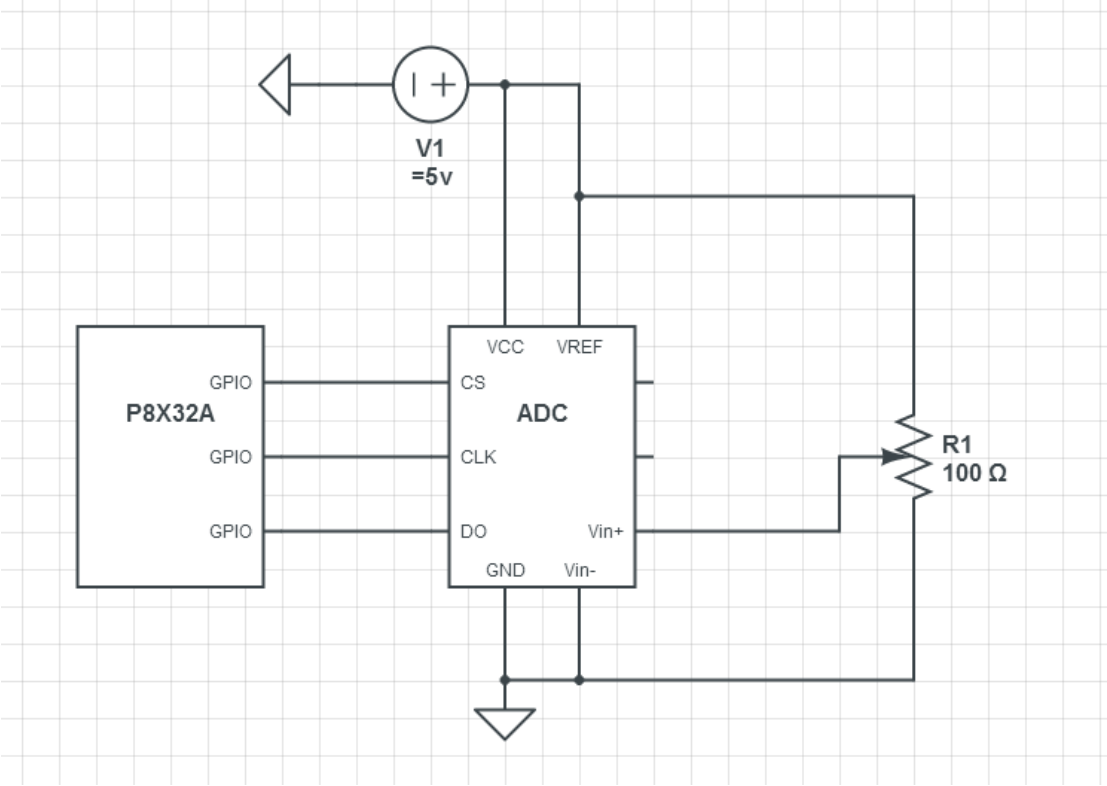

Figure 7.7: Analog Input Schematic

8.0 Speed Sensor and Display Module

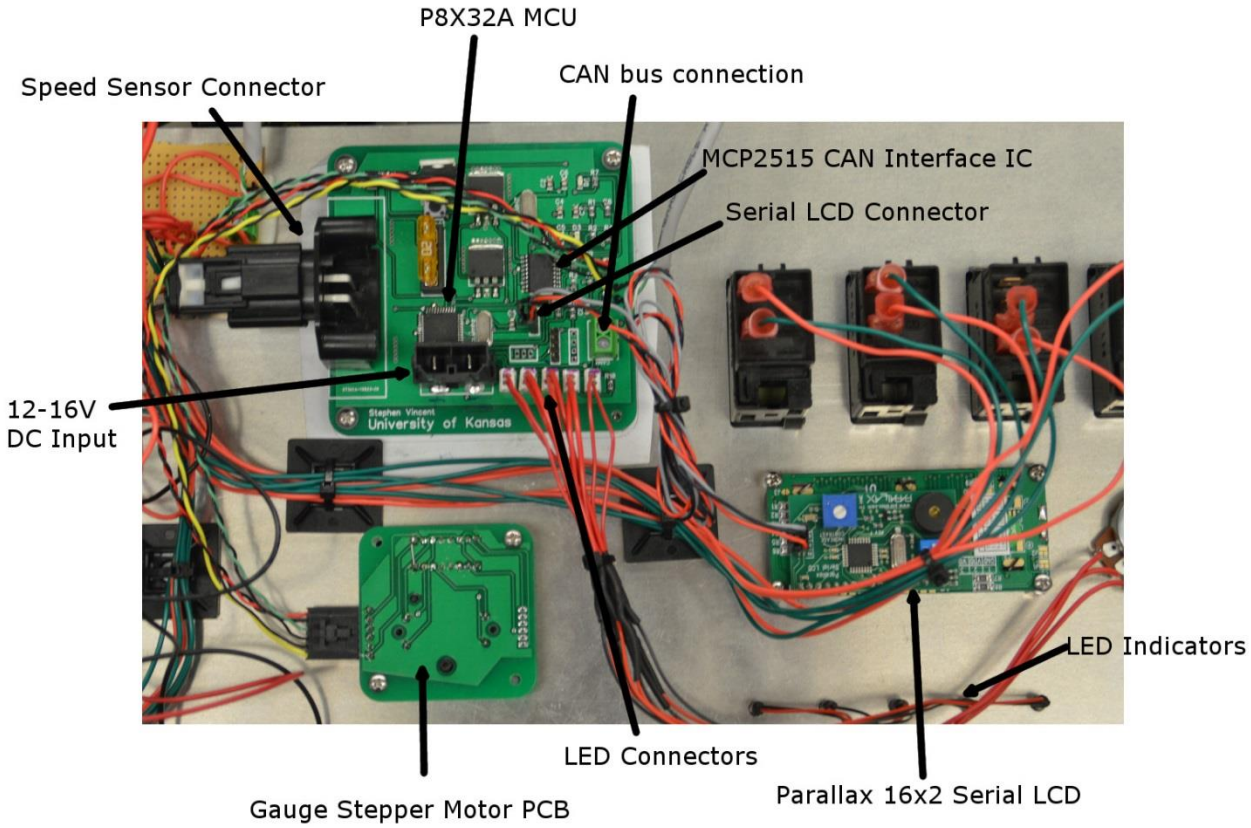

Figure 8.1: Speed Sensor and Display Module

8.1 Speed Sensor and Display Module Overview

The speed sensor and display module is responsible for measuring the vehicle's speed in miles per hour, displaying important vehicle information and transmitting speed data to the CAN bus. This module also serves the function of displaying the on/off state of certain exterior items inside the vehicle via LED's making it possible for the driver to tell the current control state of devices connected to the system. Several LED warning indicators also exist providing the driver with information on potential system malfunctions and undesirable operating conditions. Speed data is collected using a drive shaft mounted collar containing four rare earth magnets coupled

with a magnetic sensor. Display information is output to users via the use of a gauge stepper motor, 16x2 character LCD, and 5 LEDS.

8.2 Speed Sensor and Display Module System Architecture

Vehicle speed data is often acquired at either a transmission mounted Vehicle Speed Sensor (VSS) or Wheel mounted Wheel Speed Sensor (WSS). In each of these categories a number of different sensor types exist including reed switch, optical encoders, and hall-effect sensors however they all output similar digital waveforms. For this particular control system a drive shaft based system was implemented due to its ease of transfer to a different drivetrain. Transmission based VSS sensors are often specific to the transmission used. Due to the possibility of future drivetrain updates on the University of Kansas Electric Bus Platform a driveshaft based system was deemed simpler to transfer in the event of a drivetrain upgrade. The drive shaft collar used in this system comes in seven different sizes making it easy to transfer to almost any drivetrain. Four rare earth magnets are positioned inside of the collar at evenly spaced 90 degree increments. Each time one of these magnets passes in front of the reed switch, the normally open switch closes pulling the input to pin 1 low. When a magnet is not present in front of the sensor the pin is pulled high with a pull-up resistor creating a pulse in the absence of a magnet.

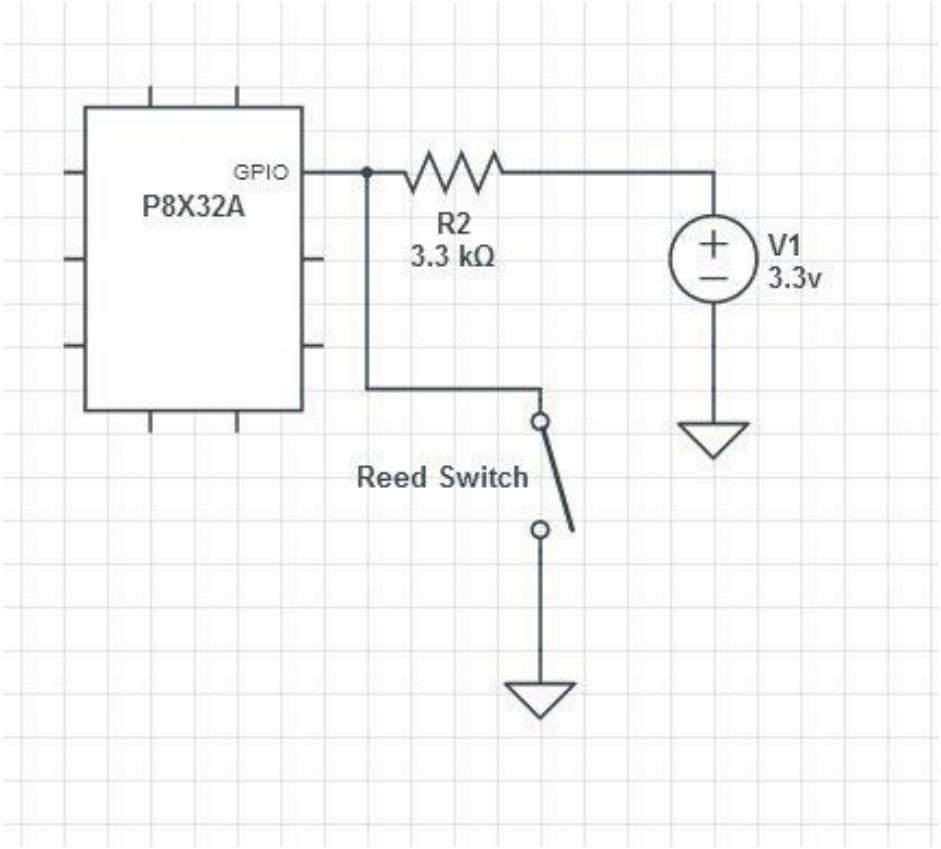

Figure 8.2: Reed Switch Schematic

As a result, each rotation of the driveshaft results in four 3.3 V pulses, which coupled with time data from the MCU can be used to calculate the drive shaft Rotations Per Minute (RPM). Assuming vehicle traction is adequate, this value will be directly proportional to vehicle speed and thus the vehicle's speed can be calculated using the data acquired by the sensor.

8.3 Speed Sensor Algorithm

Two main algorithm types exist for pulse-based speed measurement, frequency based and period based speed measurement. Frequency based speed measurement is commonly implemented by counting the number of pulses that occur in a set time increment. Period based frequency measurement is implemented by counting periods of a high frequency clock signal

that occurs within, or between, sensor pulses [23]. Frequency based systems are easy to implement but result in large amounts of error when sensors feature a low number of pulses per revolution. Error from frequency based speed measurements as a function of speed can be expressed as

$$\boldsymbol{e_w}\% = \frac{\boldsymbol{2\pi}}{\boldsymbol{\omega N_p T_{sc}}}(\boldsymbol{100}) \qquad \textbf{(Eq. 8.1)}$$

(*where* $\boldsymbol{\omega}$ *is rotational speed in radians per second,* $\boldsymbol{N_p}$ *is the number of pulses per rotation and* $\boldsymbol{T_{sc}}$ *is the time-window per measurement*) [23]. This makes a frequency based algorithm impractical for use with a sensor outputting only 4 pulses per revolution, particularly at low rpm levels. In period based algorithms the error is related to the ratio of periods between the high frequency clock signal and that of the sensor output. In this case the period of the high frequency clock signal will be that of the 80Mhz counters built into the Parallax Propeller microcontroller and the Period of the sensor output will be orders of magnitude higher and linearly related to shaft speed. In period based systems error can be calculated using equation 8.2.

$$\boldsymbol{e_w}\% = \frac{\boldsymbol{T_{hf}}}{\frac{\boldsymbol{2\pi}}{\boldsymbol{N_p\omega}} - \boldsymbol{T_{hf}}} * \boldsymbol{100} \qquad \textbf{(Eq. 8.2)}$$

(where $\boldsymbol{T_{hf}}$ *is the period of the high frequency clock signal* $\boldsymbol{N_p}$ *is the number of pulses per revolution and,* $\boldsymbol{\omega}$ *is the rotational speed in radians/second)*

Even when using refresh rates as low as 10hz a comparison of the two methods shows at both ends of the rpm spectrum a period based algorithm is desirable.

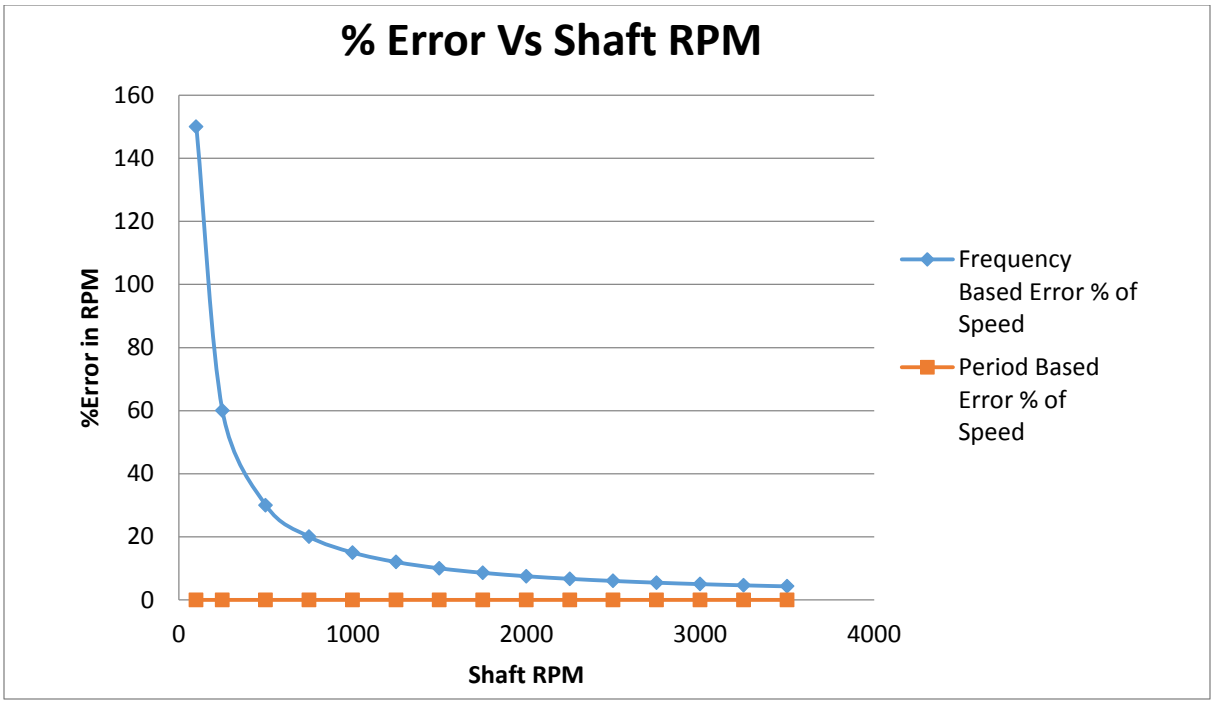

Figure 8.3: Frequency Vs Period Based Speed Error

8.4 Speed Sensor System Implementation

Due to greatly reduced error and higher refresh rate, a period based system was implemented. For this system a logic based counter was programmed to count the number of clock cycles that occur when an input pin is in the high state. The normally open reed switch allows the input pin on the microcontroller to be pulled to a high state when a magnet is not present and low when a magnet is present. Effectively, this counts the duration between magnets or the pulse width of the output signal at a very high resolution. This task is completed using the Parallax Propeller P8332A [24] hardware counter module configured in logic mode. The hardware counter module works by accumulating the number of clock cycles whenever the state of APIN is high. For this application APIN is programmed to be input pin P1 which is connected as shown in figure 8.4. In the event of a low logic state, the current value of the

PHSA Register is saved to a public variable and then reset to zero. Figure 8.4 illustrates a block diagram of the Parallax Propeller hardware counter module in Logic mode

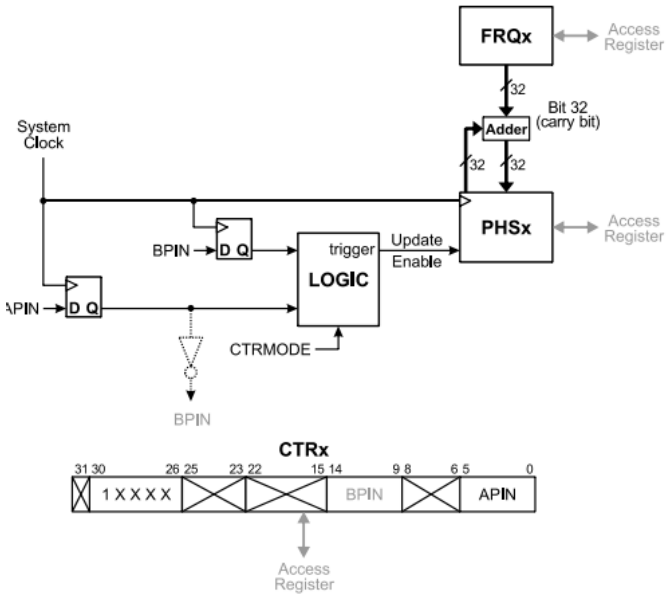

Figure 8.4: P8X32A Hardware Counter Logic Mode Block Diagram [24]

An additional benefit to using a period based system is much faster measurement. Each time a pulse is created a speed value can be calculated unlike Frequency based algorithms which feature a set time increment which much be as large as possible to reduce error.

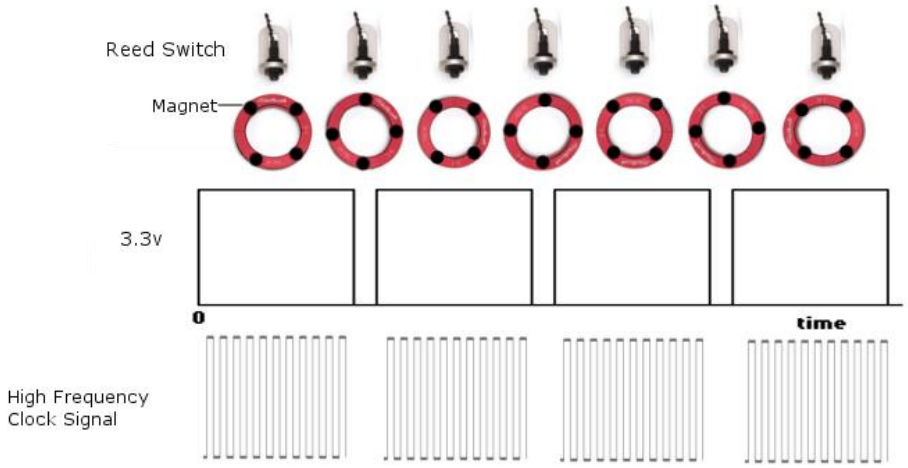

Figure 8.5: Speed Sensor Pulse Diagram

8.5 Design Concerns

8.5.1 Reed Switch Bounce

Mechanical switches transition back and forth many times very quickly before settling at their final state. This bounce often produces undesirable results since most microcontrollers are fast enough to pick up all of the transitions [25]. In the case of the speed sensor module clock cycle accumulation occurs after a transition. As a result if the system is not de-bounced the number of cycles in between bounces will be counted rather than in between pulses output from the sensor. In this particular case it was easy to apply a digital filter resetting clock cycle accumulations below a specified minimum value. This effectively removes all accumulation values in between bounces which are much lower than any accumulation values possible at speeds which a bus or vehicle will ever operate at.

8.5.2 Stopping Mid-Pulse

In the event of a complete stop it is likely that the sensor may come to rest in between two of the magnets. In this case the algorithm won't update until the sensor passes by the next magnet sending a digital low signal to the microcontroller. In order to prevent an extended pulse from preventing speed output, a function was written to limit the maximum pulse duration and output a speed of zero in the event of pulse duration's exceeding that value.

8.5.3 Calibration

Calibration was completed using a test setup capable of turning several known rotational speeds. For this sensor several milling machines were used to accurately spin the driveshaft collar at given RPM rates as well as test the sensor's ability to manage rapid acceleration.

Figure 8.6: Rotational Speed Calibration Setup

Data was recorded at 13 different points and curve fitting methods were used to obtain an equation resulting in accurate speed readings from 0-3500 rpms. Once accurate RPM measurement is established the vehicle speed can be determined by finding a linear relationship between driveshaft rotational speed and vehicle speed.

8.5.4 Display Operations

In an effort to de-clutter the dashboard while maintaining the same displayable information as the previous system as well as expandability in the event of future module development a 16x2 LCD and indicator LEDs were used to display pertinent system information. A traditional style needle gauge utilizing an automotive gauge stepper motor is used to display vehicle speed allowing operators to not only tell rough vehicle speed but rate of change as well. The gauge stepper itself was mounted to a printed circuit board with connector pins and an SN754410NE H-bridge [26] as can be seen in figure 8.7. 2.54 mm pitch connector pins are

featured on the circuit board allowing for easy wired connection to the main speed sensor module and the H-bridge IC allows for control signals at either 3.3 V or 5.0 V levels to be used as long as a 5.0 V supply connection is also present.

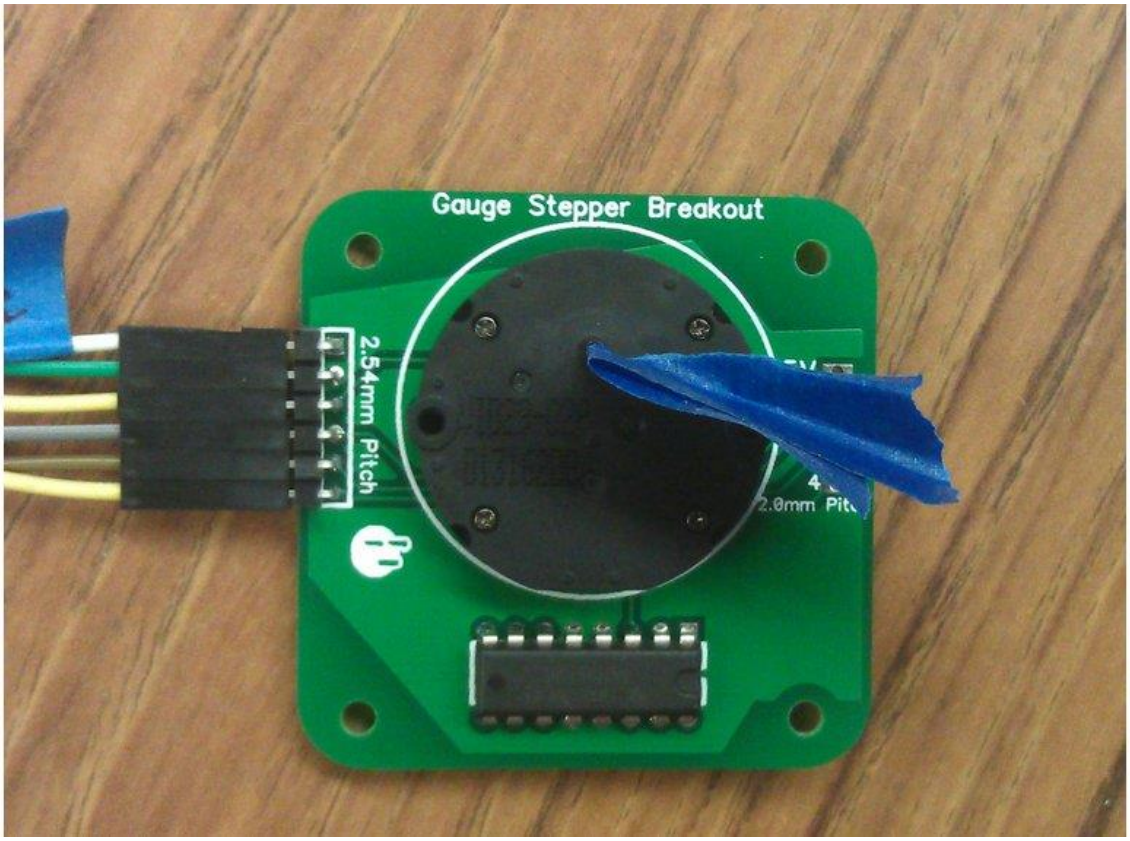

Figure 8.7: Gauge Stepper Breakout board.

The previous vehicle dashboard pictured in figure 8.8 is a dashboard originally designed for a gasoline powered bus. The gas powered version of this dashboard did not feature either of the top two circular gages, both of which are used to measure the voltage of the traction battery pack. Both gauges are off the shelf components designed to measure much lower voltages than the full system pack and only display one-tenth of the actual traction pack voltage which is measured after passing through a voltage divider. The bottom right circular gauge is a fuel gauge which is no longer necessary following the vehicles conversion to electric power.

Figure 8.8: Previous Vehicle Dashboard

Figure 8.9: CAN-Based System Dashboard

Speed display is completed using a VID model 29 gauge stepper motor [27]. This low power stepper motor is the same model used by a large number of automobile manufacturers

allowing speed to be displayed as well as information on relative rates of change in speed. A digital speed readout is also possible if the LCD screen is placed in speed display mode however many drivers still prefer an analog speed gauge to a digital speed readout due to their ability to display changes in rate of speed.

8.5.5 LCD

This system features a Parallax Model # 27977 serial LCD screen with backlight and two rows of 16 characters [28]. A serial LCD allows control using only I/O pin and asynchronous serial communication capable of working at either 2400, 9600, or 115,200 baud rate and features power consumption of only 80ma at 5v when the backlight is turned on.

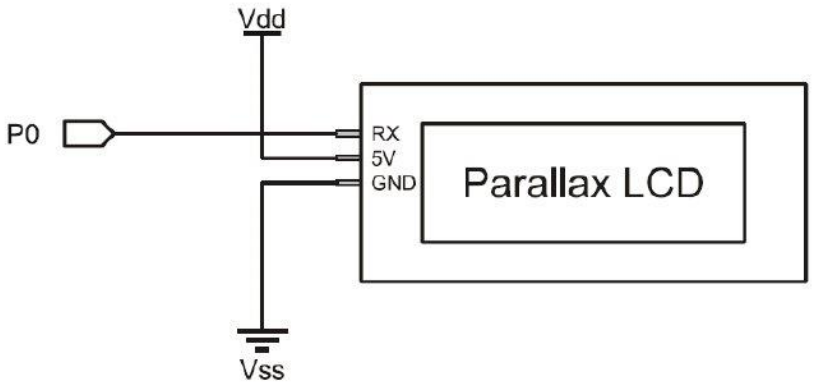

Figure 8.10: LCD Wiring

Display control is completed using simple serial commands to this LCD creating added simplification in software development allowing more processing power to be used for the module's other tasks. The mode selection switch on the dashboard allows the LCD to be switched between one of four display modes. Those modes include Speed display (miles per hour), RPM display (rotations per minute), Temperature display (degrees Fahrenheit) and traction pack voltage display (volts).

Five LEDs on the upper right hand corner of the dashboard display the current state of several bus parameters. Left to right the LEDs display the states of the following bus parameters: headlight on/off state, interior light on/off state, wiper on/off state, low traction pack voltage warning. The first three lights work illuminating the LED when that function is on and turning the LED off when it is in the off state. This feature allows drivers to diagnose possible malfunctions such as burned out bulbs or damaged wiper motors. The final two indicators blink when the warning state is reached notifying the driver that they need to either have the faulty accelerator pedal repaired or recharge the traction battery pack.

9.0 Future Development

A prototype was developed featuring one of each module type to display and test this control system. The next step in development of this project should be adding features allowing for ease of installation and maintenance followed by installation into a test vehicle. In its current state the Accelerator Pedal Sensor Module reads the state of two analog values and disables the drive functions of the bus if they are not within a programmed amount of one another. Future development in creating a limp mode preventing passengers from being stranded should also be completed.

Screw-in terminal block connectors are used for all connections to the twisted pair for the CAN bus in the current state of system development. Depending on the location of installation these connections can be difficult to make without completely removing the module. Additionally, wires can easily become dislodged resulting in lack of network connectivity to the rest of the system. Implementing a standardized connector such as a standard Ethernet cable

connector built into each module would result in much stronger connections as well as greater ease of installation.

In its current state each module used in this control system must be separately programmed using a USB connection to a PC. This works well on a test bench but may prove difficult depending on the installed locations of modules within an electric vehicle. Development of a CAN based programming system allowing all modules to be reprogrammed from one common connection point would greatly simply maintenance and upgrades to the system.

In the event that a problem is detected by the control system's computer, a beneficial development to this system would be creating a limp mode that does not strand passengers. Currently the control system is designed to disable drive capabilities when a fault is detected in the accelerator pedal position sensor. A beneficial upgrade would be a method of determining which of the two analog inputs from the accelerator position sensor is faulty allowing the vehicle to be placed in a reduced capability limp mode using the signal from the other, still functional, input.

10.0 Conclusion

This thesis documents the development and implementation of a Controller Area Network based electric vehicle control system. One of each module type was installed into a small test setup to show and demonstrate overall system functionality. Designing the system to utilize a number of different modules allows the system to be easily expanded to work in many different vehicle applications. Modules may be added and subtracted from the system in any combination allowing for a control system tailored to each specific vehicle it is used in. Another

benefit of this CAN based system is the ability to quickly and easily change system functionality by simply reprogramming modules. Since CAN is a message based protocol each module connected has access to all of the information sent over the CAN bus making it easy to add functionality without the need for any additional wiring.

References

[1] Schiffer, M. B. (2010). Taking charge : the electric automobile in America. Washington, Smithsonian Books.

[2] Westbrook, M. H., et al. (2001). The electric car : development and future of battery, hybrid, and fuel-cell cars. London Warrendale, PA, Institution of Electrical Engineers; Society of Automotive Engineers.

[3] Kirsch, D. A. (2000). The electric vehicle and the burden of history. New Brunswick, N.J., Rutgers University Press.

[4] Pazul, K. (1999). "Controller area network (can) basics." Microchip Technology Inc. Preliminary DS00713A-page 1.

[5] Corrigan, S. (2002). "Introduction to the controller area network (CAN)." Application Report, Texas Instruments.

[6] Blackman, Jason and Monroe, Scott, "Overview of 3.3v CAN (Controller Area Network) Transceivers," Texas Instruments, Application Note. SLLA337, Jan 2013.

[7] Stand-Alone, C. (1999). "Controller with SPI Interface." Microchip Technology Inc.

[8] Texas Instruments, "3.3-V CAN TRANSCEIVERS," SN65HVD230 SN65HCD231 SN65HVD232 datasheet, March 2001 [Revised February 2011].

[9] Macroblock, "Step-Down 1A LED Driver," MBI6651 datasheet, Feb 2009.

[10] Betlux, "High Power LED," BL-HP20AxxxL datasheet,

[11] Shat-R-Shield Inc., "Product Catalog & Specification Guide," http://www.shatrshield.com

[12] Panasonic Industrial Devices Sales Company of America, "General Catalog Automotive Relays," February 2013

[13] Luo, Y., et al. (2012). Study on the reliability test of automotive relays under temperature cycling condition. Electrical Contacts (ICEC 2012), 26th International Conference on.

[14] Fairchild Semiconductor, "N-Channel QFET MOSFET 60V, 32 A, 35mΩ," FQP30N06L datasheet, November 2013.

[15] Anwar, Sohel, ed. *Fault Tolerant Drive by Wire Systems*. Bentham Science Publishers, 2012.

[16] mns-drive-by-wire.jpg, Lokar Performance Products Inc. http://www.lokar.com/product-pgs/new-products/newproduct-images/drive-by-wire/mns-drive-by-wire.jpg

[17] McKay, D., et al. (2000). Delphi Electronic Throttle Control Systems for Model Year 2000: Driver Features, System Security, and OEM Benefits: ETC for the Mass Market, SAE International.

[18] Versmold, H. and M. Saeger (2006). Plausibility Checking of Sensor Signals for Vehicle Dynamics Control Systems. 8th International Symposium on Advanced Vehicle Control AVEC, Taiwan.

[19] Texas Instruments, "ADC0831-N/ADC0832-N/ADC0834-N/ADC0838-N 8-Bit Serial I/O A/D Converters with Multiplexer Options," ADC0831-N, ADC0832-N, ADC0834-N, ADC0838-N datasheet. August 1999.[Revised March 2013].

[20] Texas Instruments, "Low Power Triple and Quad Channels Digital Isolators," ISO7631FM, ISO7631FC, ISO7641FC datasheet, September 2012. [Revised September 2013].

[21] Murata Power Solutions, "3kVDC Isolated 3W Single Output DC/DC Converters," MEV3 series datasheet.

[22] Maxim Integrated, "Cold-Junction-Compensated K-Thermocouple-to-Digital Converter (0°C to +1024°C)," MAX6675 datasheet. 2002.

[23] Petrella, Roberto, et al. "Speed measurement algorithms for low-resolution incremental encoder equipped drives: a comparative analysis." *Electrical Machines and Power Electronics, 2007. ACEMP'07. International Aegean Conference on*. IEEE, 2007.

[24] Parallax Semiconductor, "Propeller P8X32A Datasheet," P8X32A datasheet, June 2011.

[25] Ganssle, J. G. (2004). "A guide to debouncing." Guide to Debouncing, Ganssle Group, Baltimore, MD, US: 1-22.

[26] Texas Instruments, "Quadruple Half-H Driver," SN754410 datasheet. November 1986. [Revised November 1995]

[27] Hong Kong VID Company Limited, "VID29 Series Stepper Motor," VID29-XX/XXP datasheet.

[28] Parallax Semiconductor, “Parallax Serial LCD,” 27976 27977 27979 datasheet, March 2013.